

Driving force on flowing quantum vortices in type-II superconductors with finite Ginzburg-Landau parameter

Shunki Sugai,^{*} Noriyuki Kurosawa[✉], and Yusuke Kato[†]

Department of Basic Science, University of Tokyo, Meguro-ku, Tokyo 153-8902, Japan

 (Received 1 February 2021; revised 18 June 2021; accepted 16 August 2021; published 30 August 2021)

The origin of the driving force on quantum vortices in superconductors has long been discussed. We investigate the origin of this force using the momentum flux tensor \mathcal{P} , Maxwell stress tensor \mathcal{T} , and numerical solutions for a flowing rectilinear vortex in the time-dependent Ginzburg-Landau (TDGL) theory for three-dimensional superconductors with finite Ginzburg-Landau parameter κ and the Maxwell equations. We calculate the hydrodynamic force $\mathbf{F}_{\text{hydro}}(C)$ and magnetic Lorentz force $\mathbf{F}_{\text{mag}}(C)$ respectively using the contour integral of \mathcal{P} and \mathcal{T} along a closed path that winds around the vortex line. The calculations show that neither $\mathbf{F}_{\text{hydro}}(C)$ nor $\mathbf{F}_{\text{mag}}(C)$ reaches the full magnitude of the driving force. However, when the path C is farther than the penetration depth from the vortex line and hence the energy dissipation is negligible on C , the sum of the two forces becomes independent of the choice of C and accounts for the full magnitude of the driving force on the vortex. We demonstrate the applicability of this result to a flowing vortex described in the generalized or modified version of the TDGL equation and to a pinned vortex. We then discuss the driving force on the Pearl vortex in two-dimensional superconductors and a curved vortex line in three-dimensional superconductors. We propose an experiment that locally probes the magnetic field with a pinned vortex to verify our results that the contribution of the magnetic pressure (Lorentz force) to the total driving force on the vortex is less than half.

DOI: [10.1103/PhysRevB.104.064516](https://doi.org/10.1103/PhysRevB.104.064516)

I. INTRODUCTION

Quantum vortices play an important role in most recent research on superconductivity, such as that on twisted bilayer graphene [1], Majorana fermions in Fe-based superconductors [2], and spintronics in superconductors [3]. A vortex in topological superconductors accommodates Majorana fermions [4], and two-dimensional (2D) superconductors undergo the Berezinskii-Kosterlitz-Thouless transition [5–8], which is induced by the dissociation of a vortex pair at high temperature. In recent research on spintronics in superconductors, the vortex spin-Hall effect was discussed [9,10], where the vortex carries spin and thus its motion is accompanied by the spin current. An understanding of vortex dynamics and a method for controlling vortices are thus of vital importance to advancements in the physics of superconductivity and its applications. A fundamental but unsettled issue related to vortices in superconductors, which is addressed in the present study, is the origin of the driving force on a single vortex in the presence of an external current [11–22]. Many reviews and textbooks [22–29] state that a single vortex located at \mathbf{r} in the presence of a transport current $\mathbf{j}_{\text{tr}}(\mathbf{r})$ is subjected to the driving force \mathbf{F}_{drv} (per unit length along the vortex axis), which is expressed as

$$\mathbf{F}_{\text{drv}} = \mathbf{j}_{\text{tr}}(\mathbf{r}) \times \boldsymbol{\phi}_0, \quad (1)$$

where $\boldsymbol{\phi}_0$ is the vector parallel to the magnetic field at the vortex center and $|\boldsymbol{\phi}_0|$ is $h/(2|e|)$, with h being the Planck constant and $|e|$ being the unit charge. In the following, we take the charge of Cooper pair $e^* = 2|e|$ to be positive for simplicity. For a pinned vortex, the driving force Eq. (1) is balanced by the pinning force \mathbf{F}_{pin} (per unit length along the vortex axis):

$$\mathbf{F}_{\text{drv}} + \mathbf{F}_{\text{pin}} = 0. \quad (2)$$

For a flowing vortex, it is balanced by the environmental force [28]:

$$\mathbf{F}_{\text{drv}} + \mathbf{F}_{\text{env}} = 0. \quad (3)$$

\mathbf{F}_{env} has the general form

$$\mathbf{F}_{\text{env}} = -\eta_1 \mathbf{v} + \eta_2 \mathbf{e}_z \times \mathbf{v}, \quad \eta_1 > 0. \quad (4)$$

Here, \mathbf{v} denotes the velocity of the vortex and \mathbf{e}_z is the unit vector parallel to the z axis, which we take as the direction of the magnetic field. The force balance relation Eq. (3) with the expressions for η_1 in Eq. (4) has been derived with the time-dependent Ginzburg-Landau (TDGL) and generalized TDGL equations [28,30], Usadel equations [31], and quasiclassical theory for superconductivity [32–34]. The force balance relation with η_1 and η_2 was given in [35,36]. In this method [33,34], Eq. (3) with Eq. (4) is derived from the solvability condition of inhomogeneous linear equations without solving the equations themselves. To address the origin of the driving force, however, it is necessary to solve the equations used to calculate the flow state of the vortex. No consensus has been reached regarding the origin of the driving force Eq. (1)

^{*}sugai@vortex.c.u-tokyo.ac.jp

[†]yusuke@phys.c.u-tokyo.ac.jp

[11–21], which is often referred to as the Lorentz force in review articles and monographs [28,34]. Several authors [16,17] have argued that Eq. (1) is of hydrodynamic origin in the type-II limit (where the penetration depth λ is much longer than the coherence length ξ). Other authors [19,21] have argued that the driving force consists of hydrodynamic and magnetic contributions. One reason for this lack of consensus is the lack of an experiment that could demonstrate which theory is correct. Another reason is that a direct method to calculate the force on a pinned vortex is not applicable to a flowing vortex. The force on the pinned vortex can be obtained by derivative of the interaction energy or potential energy [37] but the force on the flowing vortex cannot. In the presence of dissipation, it is legitimate to calculate the force on the flowing vortex based on the local momentum balance relation.

One of the present authors and Chung previously investigated the origin of the driving force on vortices in superconductors [21] based on the local momentum balance relation and hydrodynamic and Maxwell stresses. In the present study, we investigate the origin of the driving force using the fully solved TDGL and Maxwell equations up to the linear response to the transport current. We then propose an experiment for confirming the origin of the driving force. We also extend our discussion to other types of TDGL equations and the Pearl vortex [38] in 2D superconductors.

The rest of this paper is organized as follows. In the next section, we explain the underlying properties of the well-defined force on vortices and define the driving force, the pinning force, and the environmental force. In Sec. III, we explain the TDGL equation, the local balance relation and boundary condition, and the numerical calculation method. In Sec. IV, we present the numerical results for the current density, electromagnetic field, local hydrodynamic force, local magnetic Lorentz force, dissipation function, energy flow, and the driving force on the vortex. In Sec. V, we discuss the validity of our results on the driving force on quantum vortices in various types of TDGL models and for a pinned vortex. Among these cases, we study the driving force on the vortex in 2D superconductors (i.e., the Pearl vortex) in detail in Sec. VI. In Sec. VII, we discuss the relation between the driving force and the topological number that characterizes vortices. We also remark on the Berry phase approach for deriving the driving force on vortices. We further propose an experiment for verifying some of our results and discuss future issues. In Sec. VIII, we summarize our results and give the conclusions. In Appendix A, we present the calculation and a discussion of the driving force on a deformed vortex line. In Appendix B, we explain the details of the calculation for the Pearl vortex.

II. PRELIMINARIES

We first briefly review the Magnus force on a narrow cylindrical object in a classical ideal fluid as a prototype of the force on various kinds of vortex. An object immersed in a uniform flow is subjected to the Magnus force when the circulation around the object is nonzero. This force is defined by the contour integral of the normal component of the momentum flux tensor $\mathcal{P}_{\mu\nu}$ [$= \rho(v_\mu v_\nu - v^2 \delta_{\mu\nu}/2)$] along

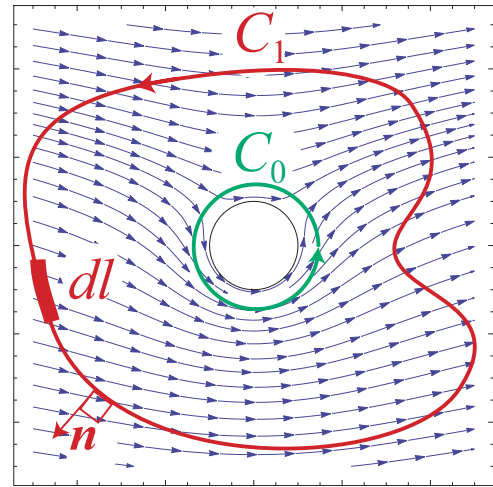


FIG. 1. Flow of ideal fluid around an object. Circulation is positive and thus this object is subjected to the Magnus force.

the closed path C surrounding the object:

$$\mathbf{F}(C)_\mu = - \oint_C d\ell \mathcal{P}_{\mu\nu} n_\nu. \quad (5)$$

The right-hand side of Eq. (5) expresses the momentum flowing into the region S surrounded by the closed loop C . Owing to the divergence-free property $\partial_\nu \mathcal{P}_{\mu\nu} = 0$ in an ideal fluid, the right-hand side of Eq. (5) is path-independent so long as the closed path has the same winding number ($=1$ in the present case). Due to this path independence of Eq. (5), the net force on the fluid particles in the region between C_1 and C_0 is zero in Fig. 1 and thus the force $\mathbf{F}(C_1)$ acts only on the object.

Now we turn to superconductors and consider the Maxwell stress (magnetic pressure) acting on the region S , which contains an isolated flowing/pinned vortex.

$$[\mathbf{F}_{\text{mag}}(C = \partial S)]_\mu = \oint_C d\ell \mathcal{T}_{\mu\nu} n_\nu, \quad (6)$$

$$\mathcal{T}_{\mu\nu} = \frac{1}{\mu_0} \left(h_\mu h_\nu - \frac{\delta_{\mu\nu}}{2} \mathbf{h}^2 \right).$$

Here, $\mathcal{T}_{\mu\nu}$ denotes the magnetic part of the Maxwell stress tensor and $\mathbf{h} = \mathbf{h}(\mathbf{r})$ denotes the local magnetic field. The right-hand side of Eq. (6) expresses the momentum flow (of the magnetic field) into the region S surrounded by the closed loop C . In contrast to the momentum flux tensor in an ideal fluid, the divergence of the Maxwell stress tensor $\partial_\nu \mathcal{T}_{\mu\nu} = (\mathbf{j} \times \mathbf{h})_\mu$ is not zero and thus $[\mathbf{F}_{\text{mag}}(C)]_\mu$ is *path-dependent* and thereby cannot be regarded as a force on the vortex.

Next, we consider the hydrodynamic momentum flow into the region S in the superconductor. It can be expressed in the same way as Eq. (5) but the expression and the property for the momentum flux tensor are different for superconductors [the expression for $\mathcal{P}_{\mu\nu}$ in the TDGL equation for superconductors is given later in Eq. (26)]. In superconductors, the momentum flux tensor $\mathcal{P}_{\mu\nu}$ is not divergence-free; that is, $\partial_\nu \mathcal{P}_{\mu\nu} \neq 0$. The hydrodynamic pressure Eq. (5) in superconductors is path-dependent and thus cannot be regarded as a force on the vortex. However, when C is sufficiently far from

the vortex core [21], the sum of the magnetic and hydrodynamic pressures in superconductors becomes divergence-free:

$$\partial_\nu(\mathcal{T}_{\mu\nu} - \mathcal{P}_{\mu\nu}) = 0. \quad (7)$$

This divergence-free condition holds outside the region where energy dissipation occurs for a flowing vortex. For a pinning vortex, the divergence-free condition holds in the region where the pinning force on the vortex is negligible. The relation Eq. (7) was called the stress-free condition in [39]. The force

$$[\mathbf{F}_{\text{tot}}(C)]_\mu = \oint_C d\ell(\mathcal{T}_{\mu\nu} - \mathcal{P}_{\mu\nu})n_\nu \quad (8)$$

is path-independent and thus Eq. (8) can be regarded as a force on the vortex in superconductors so long as C belongs to the stress-free region. As stated in a review article [22] (see page 1130 in the reference), this is a strict way to define the force of the (driving) force on vortices in superconductors in terms of the momentum flux tensor and Maxwell stress tensor to discuss the origin of the driving force.

For clarity, we more explicitly define the driving force and the environmental force. Let $\mathbf{g}(\mathbf{r}, t)$ be the momentum density and suppose that the momentum balance relation for superconductors in the lattice frame is given in the form

$$\frac{\partial \mathbf{g}(\mathbf{r}, t)}{\partial t} + \nabla \cdot \mathbf{\Pi}(\mathbf{r}, t) = -\mathbf{f}(\mathbf{r}, t), \quad (9)$$

where $\mathbf{\Pi}(\mathbf{r}, t)$ is a second-rank tensor and the right-hand side represents the momentum transfer to the background or pinning center. When

$$\oint_C d\ell \mathbf{\Pi}(\mathbf{r}, t) \cdot \mathbf{n} \quad (10)$$

for the closed path C , which winds around the vortex and belongs to the stress-free region, is independent of the path, we define the driving force on the vortex as

$$\mathbf{F}_{\text{drv}}(t) := - \oint_C d\ell \mathbf{\Pi}(\mathbf{r}, t) \cdot \mathbf{n}. \quad (11)$$

When the right-hand side of Eq. (9) represents the irreversible momentum transfer to the background, the environmental force on the vortex is defined by

$$\mathbf{F}_{\text{env}}(t) := - \int_S dS \mathbf{f}(\mathbf{r}, t) \quad (12)$$

with the 2D region S such that $\partial S = C$. When the right-hand side of Eq. (9) represents the reversible momentum transfer to the pinning center, the pinning force on the vortex is defined by

$$\mathbf{F}_{\text{pin}}(t) := - \int_S dS \mathbf{f}(\mathbf{r}, t). \quad (13)$$

However, there is no consensus on how the force that originates from

$$\int_S \frac{\partial \mathbf{g}(\mathbf{r}, t)}{\partial t} \quad (14)$$

should be categorized. Because this is a matter of semantics, we assign (14) to neither the driving force, environmental force, nor pinning force.

III. MODEL

We introduce the TDGL equation [40,41] in Sec. III A and present the local balance relations (energy balance and momentum balance) in Sec. III B. The momentum balance relation plays a key role throughout this paper. In Sec. III C, we present the boundary value problem for a flowing single vortex. In Sec. III D, we briefly summarize the numerical methods. The details of the numerical methods are explained in the Supplemental Material [42].

A. TDGL equation

The TDGL equation is the simplest model of a vortex based on microscopic theory [40,41]. We make the order parameter $\psi = f(\mathbf{r}, t)e^{i\chi(\mathbf{r}, t)}$ dimensionless so that an equilibrium solution in the bulk becomes $f = 1$ with a constant χ . It is convenient to introduce the gauge-invariant scalar P and vector \mathbf{Q} potentials as

$$P = \Phi + \frac{\hbar}{e^*} \frac{\partial \chi}{\partial t}, \quad \mathbf{Q} = \mathbf{A} - \frac{\hbar \nabla \chi}{e^*}, \quad (15)$$

where Φ is the electrochemical potential divided by $e^* = 2|e|$ and the vector potential \mathbf{A} . The electric field (including the gradient of the chemical potential) and magnetic field are respectively expressed as $\mathbf{e} = -\partial_t \mathbf{Q} - \nabla P$ and $\mathbf{h} = \nabla \times \mathbf{Q}$ for any position except the vortex center. The TDGL equation can be written in terms of f , P , and \mathbf{Q} as

$$\gamma \frac{\partial f}{\partial t} = \xi^2 \nabla^2 f - \left(\frac{e^* \xi \mathbf{Q}}{\hbar} \right)^2 f + f - f^3, \quad (16a)$$

$$\nabla \cdot f^2 \mathbf{Q} = - \frac{\gamma f^2 P}{\xi^2}, \quad (16b)$$

where the relaxation time $\gamma > 0$ for the order parameter. The equations are coupled with the Ampère law

$$\nabla \times \mathbf{h} = \mu_0 \mathbf{j}, \quad (17)$$

where the current density \mathbf{j} consists of two parts:

$$\mathbf{j} = \mathbf{j}_s + \mathbf{j}_n, \quad \mathbf{j}_s = - \frac{f^2 \mathbf{Q}}{\mu_0 \lambda^2}, \quad \mathbf{j}_n = \sigma_n \mathbf{e}. \quad (18)$$

Here, \mathbf{j}_s and \mathbf{j}_n are respectively the supercurrent density and normal current density. The symbol σ_n denotes the Ohmic dissipative conductivity.

The system of equations has two characteristic length scales, namely λ and ξ , and two characteristic timescales, namely γ and $\sigma_n \mu_0 \xi^2$, for the relaxation process. With the dimensionless quantity

$$\zeta = \left(\frac{\sigma_n \mu_0}{\gamma} \right)^{\frac{1}{2}} \xi, \quad (19)$$

the characteristic length scale for the electrochemical potential is given by $\zeta \lambda =: \ell_p$. With the unit $v_0 = 1/(\sigma_n \mu_0 \lambda)$, we can measure the vortex velocity.

B. Local balance relations

The energy balance relation for Eqs. (17), (16a), and (16b) is given by [28,43]

$$\frac{\partial}{\partial t} \left(\frac{B^2}{2\mu_0} + \mathcal{F}_{\text{sn}} \right) + \nabla \cdot \mathbf{j}_E = -W \quad (20)$$

with

$$\mathcal{F}_{\text{sn}} \equiv \frac{Q^2}{2\mu_0\lambda^2} + \frac{B_c^2}{\mu_0} \left\{ \xi^2 |\nabla f|^2 - f^2 + \frac{f^4}{2} \right\}, \quad (21)$$

the energy current density

$$\mathbf{j}_E = \left[\frac{\mathbf{e} \times \mathbf{h}}{\mu_0} + \frac{P f^2 Q^2}{\mu_0 \lambda^2} - \left(\frac{\hbar}{e^*} \right)^2 \frac{1}{\mu_0 \lambda^2} \frac{\partial f}{\partial t} \nabla f \right], \quad (22)$$

and the local dissipation function

$$W = \sigma_n \mathbf{e}^2 + \tilde{\gamma} \left(\frac{e^* f P}{\hbar} \right)^2 + \tilde{\gamma} \left(\frac{\partial f}{\partial t} \right)^2. \quad (23)$$

Here, we introduce the notation

$$\tilde{\gamma} = \frac{2B_c^2}{\mu_0} \gamma, \quad B_c = \frac{|\phi_0|}{2\sqrt{2\pi} \lambda \xi}. \quad (24)$$

The expression for W can be used to determine the strength and distribution of the energy dissipation in the flowing vortex state. The momentum balance relation, shown below, follows from Eqs. (17), (16a), and (16b):

$$\begin{aligned} \partial_\nu (-\mathcal{P}_{\mu\nu} + T_{\mu\nu}) + \tilde{\gamma} \partial_\mu f \partial_t f - \tilde{\gamma} (2\pi/\phi_0)^2 f^2 P Q_\mu \\ - (\mathbf{j}_n \times \mathbf{h})_\mu = 0. \end{aligned} \quad (25)$$

See [21] for derivation of Eq. (25). The tensor $\mathcal{P}_{\mu\nu}$, expressed as

$$\mathcal{P}_{\mu\nu} = \frac{f^2 Q_\mu Q_\nu}{\mu_0 \lambda^2} + \frac{2B_c^2 \xi^2}{\mu_0} \partial_\nu f \partial_\mu f - \delta_{\mu\nu} \mathcal{F}_{\text{sn}}, \quad (26)$$

can be considered as the momentum flux tensor. In the London approximation (f is fixed to be unity),

$$\begin{aligned} \mathcal{P}_{\mu\nu} &\rightarrow \frac{1}{\mu_0 \lambda^2} \left(Q_\mu Q_\nu - \delta_{\mu\nu} \frac{Q^2}{2} \right) + \delta_{\mu\nu} \frac{B_c^2}{2\mu_0} \\ &= \mu_0 \lambda^2 \left(j_{s,\mu} j_{s,\nu} - \delta_{\mu\nu} \frac{j_s^2}{2} \right) + \delta_{\mu\nu} \frac{B_c^2}{2\mu_0}, \end{aligned} \quad (27)$$

which is similar to the momentum flux tensor for an ideal fluid. From Eqs. (23) and (25), we see that in the region

where $W = 0$ (dissipation-free region), the divergence-free condition Eq. (7) holds for the TDGL equation.

C. Boundary value problem of flowing state of single vortex

We consider a superconducting system with infinite extension along the x and z axes but with a finite thickness along the y axis, $y \in [-\ell_y, \ell_y]$. We take the direction of the magnetic field in equilibrium to be along the z axis and the direction of transport current far from the vortex to be along the x axis. All physical quantities are assumed to be uniform along the z axis. The half thickness ℓ_y is a few times the penetration depth so that the effect of the image vortex is negligible. We set the (spatially varying) transport current density near the boundary to be much smaller than the critical current density. We can then obtain the solution for boundary value problems by solving the same equations for systems with infinite extension along y with an accuracy on the linear order of the transport current. At the end of the next subsection, we evaluate the condition on the value of ℓ_y and the magnitude of the transport current for our approach to be valid.

We denote the vortex velocity by \mathbf{v} and set the corresponding flux flow solution in the form of the sum of the rigid translation and the deformation:

$$\begin{aligned} X(\mathbf{r}, t) &= X_0(\mathbf{r} - \mathbf{v}t) + X_1(\mathbf{r}) + \mathcal{O}(v^2), \\ X &= f, Q, P, \dots \end{aligned} \quad (28)$$

Here, $X_0(\mathbf{r})$ is the equilibrium solution (note that $P_0 = 0$). The asymptotic forms of $\mathbf{Q}_0(\mathbf{r})$ and $\mathbf{h}_0(\mathbf{r})$ for $r \gg \xi$ are given by (e.g., [44])

$$\mathbf{Q}_0(\mathbf{r}) \sim -\frac{c(\kappa)|\phi_0|K_1(r/\lambda)}{2\pi\lambda} \mathbf{e}_\theta = Q_0(r) \mathbf{e}_\theta, \quad (29)$$

$$\mathbf{h}_0(\mathbf{r}) \sim \frac{c(\kappa)|\phi_0|K_0(r/\lambda)}{2\pi\lambda^2} \mathbf{e}_z. \quad (30)$$

Here, the factor $c(\kappa)$ is unity in the London limit but $c(\kappa) \sim 1.086$ for $\kappa = 3$, 1.039 for $\kappa = 5$, 1.023 for $\kappa = 7$, and 1.013 for $\kappa = 10$. K_0 (K_1) denotes the second kind of modified Bessel function of the zeroth (first) order. With the notation

$$X_v(\mathbf{r}) := -\mathbf{v} \cdot \nabla X_0(\mathbf{r}), \quad X = f, Q, P, \dots, \quad (31)$$

the boundary value problems for $f_1(\mathbf{r})$, $\mathbf{Q}_1(\mathbf{r})$, and $P_1(\mathbf{r})$ are expressed as

$$\nabla^2 P_1 - \frac{f_0^2 P_1}{\ell_P^2} = \nabla \cdot \mathbf{Q}_v = 0, \quad (32a)$$

$$LX = \mathbf{g}, \quad (32b)$$

$$L = \begin{pmatrix} H_f, & -f_0 \mathbf{Q}_0 / (\mu_0 \lambda^2) \\ -f_0 \mathbf{Q}_0 / (\mu_0 \lambda^2), & -(\mathbf{rot} \mathbf{rot} + \lambda^{-2} f_0^2) / (2\mu_0) \end{pmatrix}, \quad (32c)$$

$$\mathbf{X} = \begin{pmatrix} f_1 \\ \mathbf{Q}_1 \end{pmatrix}, \quad \mathbf{g} = -\frac{1}{2} \begin{pmatrix} \tilde{\gamma} f_v \\ \mathbf{j}_n \end{pmatrix}, \quad (32d)$$

$$H_f = \frac{B_c^2}{\mu_0} \left[\xi^2 \nabla^2 - \left(\frac{e^* \xi \mathbf{Q}_0}{\hbar} \right)^2 + 1 - 3f_0^2 \right] \quad (32e)$$

under the boundary conditions

$$\boldsymbol{\varepsilon}_1(r \ll \lambda) < +\infty, \quad \boldsymbol{\varepsilon}_1(r \gg \lambda) \rightarrow 0, \quad (33a)$$

$$|f_1(\mathbf{r} \rightarrow 0)| < \infty, \quad f_1(\mathbf{r} \gg \xi) \sim 0, \quad (33b)$$

$$|\mathbf{h}_1(\mathbf{r} \rightarrow 0)| < \infty, \quad \mathbf{h}_1(\mathbf{r} \gg \xi) \sim \mu_0 \lambda (j_+ e^{y/\lambda} - j_- e^{-y/\lambda}) \mathbf{e}_z, \quad (33c)$$

$$|j_1(\mathbf{r} \rightarrow 0)| < \infty, \quad j_1(\mathbf{r} \gg \xi) \sim (j_+ e^{y/\lambda} + j_- e^{-y/\lambda}) \mathbf{e}_x \equiv \mathbf{j}_{\text{tr}}(\mathbf{r}), \quad (33d)$$

which sets the transport current in the x direction far from the vortex core. The boundary value problem Eq. (32b) has a solution only when the inhomogeneous term \mathbf{g} satisfies the following condition (solvability condition):

$$c(\kappa) \mathbf{j}_{\text{tr}}(\mathbf{0}) \times \boldsymbol{\phi}_0 = \tilde{\gamma} \int d\mathbf{r} [\nabla f f_v + (2\pi/|\phi_0|)^2 f^2 P_1 \mathbf{Q}_0] + \int d\mathbf{r} \mathbf{j}_n \times \mathbf{h}. \quad (34)$$

The integral on the right-hand side is taken over the entire 2D plane. We discuss this relation (34) at the end of this subsection.

The right-hand side is determined by \mathbf{v} , f_0 , \mathbf{Q}_0 , P_1 , and $\boldsymbol{\varepsilon}_1$. P_1 and $\boldsymbol{\varepsilon}_1$ are proportional to \mathbf{v} . Thus, the condition Eq. (34) imposes a relation between \mathbf{v} and parameter $j_+ + j_- = |\mathbf{j}_{\text{tr}}(\mathbf{0})| =: j_{\text{tr}}$ in the boundary conditions.

The procedure for solving the flux flow state is as follows:

- (1) Set \mathbf{v} so that the relation Eq. (34) holds for a given boundary condition.
- (2) Solve Eq. (32a) under the boundary condition Eq. (33a) to obtain P_1 .
- (3) Obtain $\boldsymbol{\varepsilon}_1$ from Eq. (33a) and obtain \mathbf{j}_n from Eq. (18).
- (4) Solve Eq. (32b) under the boundary conditions Eqs. (33b)–(33d) and obtain f_1 and \mathbf{Q}_1 .

We now discuss the solvability condition Eq. (34). This relation can be derived in essentially the same way as those for the solvability condition in earlier studies [30,35] for the large- κ case. Equation (34) is different from those in earlier studies in two ways. In earlier studies, the factor $c(\kappa)$ was set to unity because $c(\kappa \rightarrow \infty) = 1$ and $\mathbf{j}_{\text{tr}}(\mathbf{0})$ was replaced by a uniform supercurrent density far away from the vortex in the type-II limit.

The procedure for deriving Eq. (34) can be summarized as follows:

- (1) Solve Eq. (32a) under the boundary condition Eq. (33a) and obtain P_1 .
- (2) Obtain $\boldsymbol{\varepsilon}_1$ from Eq. (33a) and obtain \mathbf{j}_n from Eq. (18).
- (3) Integrate the inner product between Eq. (32b) and the zero mode over the disk region with the vortex core as the center. Perform partial integration using the boundary conditions Eqs. (33b)–(33d) and obtain the transport relation.

Note that the current density $\mathbf{j}_{\text{tr}}(\mathbf{0})$ on the left-hand side of Eq. (34) in the present case is a subtle quantity [21]; it is not the local value of the current density at the vortex core but rather a value extrapolated into the vortex core from the region far from the vortex core [see Fig. 2(a)] via the London equation. For a given state with a flowing vortex located at $\mathbf{r} = 0$ [Fig. 2(a)], we can prepare the transport current state [Fig. 2(b)] with the same current density as that of the state with the vortex [Fig. 2(a)] in the remote region from the vortex

core. Then, $\mathbf{j}_{\text{tr}}(\mathbf{0})$ is just the local current density $\mathbf{j}(\mathbf{0})$ at $\mathbf{r} = 0$ in the transport current state.

Note that the right-hand side of Eq. (34) is the same as that of the momentum balance relation Eq. (25) and it thus follows that

$$\lim_{R \rightarrow \infty} \oint_{|r|=R} (\mathcal{T}_{\mu\nu} - \mathcal{P}_{\mu\nu}) n_\nu d\ell \rightarrow c(\kappa) (\mathbf{j}_{\text{tr}}(\mathbf{0}) \times \boldsymbol{\phi}_0)_\mu, \quad (35)$$

which implies that the expression Eq. (1) for the driving force in superconductors with $\kappa \gg 1$ should have a multiplicative factor $c(\kappa)$ for superconductors with finite κ . The existence of this multiplicative factor has been discussed for the vortex-vortex two-body interaction [45].

D. Summary of numerical methods

First, we numerically obtain the equilibrium solution to $f_0(r)$ and $A_0(r)$ via an iteration method (note that the shooting method with the Runge-Kutta method is inadequate). The

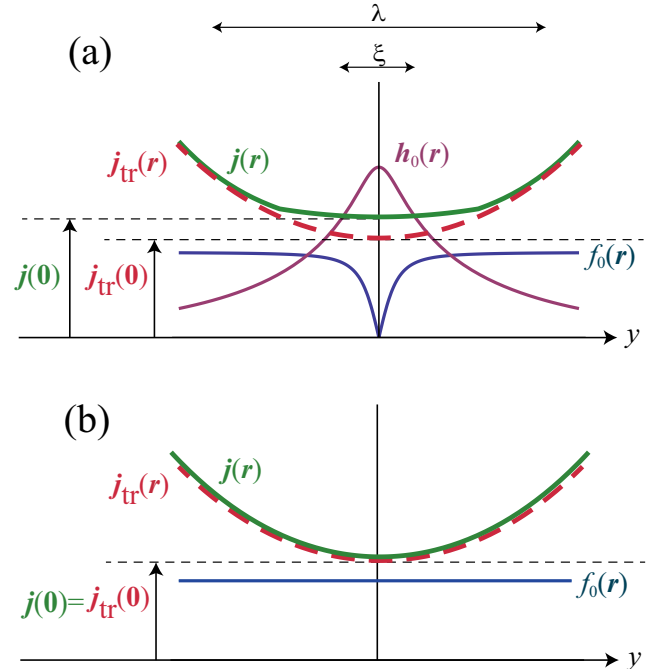


FIG. 2. (a) Schematic diagram of the order parameter, the current density, and magnetic field around a single vortex located at $\mathbf{r} = \mathbf{0}$. Green solid line denotes the current density on the plane $x = 0$. Pink dotted line denotes the current density in the absence of a vortex. These lines have common asymptotes. Blue-violet and blown lines, respectively, represent the modulus of order parameter and magnetic field. (b) Order parameter and current density in the absence of a vortex. Pink dotted line is the same as that in (a).

operator $\nabla^2 - f_0^2/\ell_p^2$ acting on P_1 in Eq. (32a) and the operator L acting on X in Eq. (32d) are axisymmetric and thus Eqs. (32a) and (32d) can be solved separately in each sector for $f_1(\mathbf{r})$, $\mathbf{Q}_1(\mathbf{r})$, $P_1(\mathbf{r})$ with a definite angular momentum ($= m$) around the z axis. The boundary value problem for each partial wave is solved numerically via hybrid series expansion near the core and the Runge-Kutta method in other regions. In the Supplemental Material [42], we explain the reduction to a one-dimensional problem in the radial direction for each partial wave and the procedure to solve the boundary value problem. We retained partial waves up to the angular momentum $m = 9$ and found that it is sufficient to retain partial waves up to the angular momentum $m = 5$.

We consider the case with $j_+ = j_- = j_{\text{tr}}/2$, where only odd m contribute.

In the next section, the numerical results are presented in the following units:

$$\sqrt{2}B_c = \frac{\hbar}{e^* \lambda \xi}, \text{ for } \mathbf{h}(\mathbf{r}), \mathbf{h}_0(\mathbf{r}), \quad (36a)$$

$$\frac{\sqrt{2}vB_c}{v_0}, \text{ for } \mathbf{h}_1(\mathbf{r}), \quad (36b)$$

$$\sqrt{2}vB_c, \text{ for } \boldsymbol{\varepsilon}(\mathbf{r}), \quad (36c)$$

$$\frac{\sqrt{2}B_c}{\mu_0 \lambda} =: j_c, \text{ for } \mathbf{j}(\mathbf{r}), \mathbf{j}_0(\mathbf{r}), \quad (36d)$$

$$\frac{\sqrt{2}vB_c}{\mu_0 \lambda v_0}, \text{ for } \mathbf{j}_1(\mathbf{r}). \quad (36e)$$

The dimensionless parameters are $\kappa (= \lambda/\xi) = 3, 5, 7, 10$, $\zeta = 1/3$, and $v/v_0 = 0.003$ for all figures but $v/v_0 = 0.05$ for Fig. 5.

We present the results for $r \leq \lambda$ on the basis of calculations for systems with infinite extension along the y , x , and z directions. However, we can interpret them as the results for systems with finite thickness $2\ell_y$ along the y direction if our solution approximately satisfies the boundary condition

$$|j_y(\mathbf{r})|_{y=\ell_y} \ll j_c. \quad (37)$$

Our results are the solutions to the TDGL and Maxwell equations up to $O(j_{\text{tr}})$ and thus valid when $|j_{\text{tr}}(y = \pm\ell_y)|$ is much smaller than the critical current density, i.e.,

$$j_{\text{tr}} e^{\ell_y/\lambda} \ll j_c. \quad (38)$$

For each value of κ , the conditions Eqs. (37) and (38) hold within an error of 1% when

(i) for $\kappa = 3$, $\ell_y/\lambda \sim 2.3$ and $j_{\text{tr}}/j_c < 1.0 \times 10^{-3}$, $v/v_0 < 8.4 \times 10^{-4}$;

(ii) for $\kappa = 5$, $\ell_y/\lambda \sim 2.1$ and $j_{\text{tr}}/j_c < 1.3 \times 10^{-3}$, $v/v_0 < 1.4 \times 10^{-3}$;

(iii) for $\kappa = 7$, $\ell_y/\lambda \sim 1.8$ and $j_{\text{tr}}/j_c < 1.8 \times 10^{-3}$, $v/v_0 < 2.2 \times 10^{-3}$;

(iv) for $\kappa = 10$, $\ell_y/\lambda \sim 1.5$ and $j_{\text{tr}}/j_c < 2.2 \times 10^{-3}$, $v/v_0 < 3.3 \times 10^{-3}$.

IV. NUMERICAL RESULTS

In Sec. IV A, we present the results for the current density, electromagnetic fields, and the order parameter as the

basic quantities of the system. We also present the results for a backflow around the vortex core to confirm the validity of our result through a comparison with an earlier result. In Sec. IV B, we show the results for local force densities, namely the local magnetic Lorentz force density and the local hydrodynamic force density. We also present the energy flow and dissipation function. Finally, in Sec. IV C, we show the momentum flow into the region that contains the vortex. We take the region to be a cylinder with the axis as the vortex line. The results show that the sum of the two forces is independent of the radius R of the cross section of the cylindrical region when $R > \lambda$.

A. Current density, electromagnetic fields, and order parameter

Figure 3(a) shows the spatial distribution of the current density $\mathbf{j}_0(\mathbf{r})$ (arrows) and $\mathbf{h}_0(\mathbf{r})$ (density plot) in equilibrium. Figure 3(b) shows $\mathbf{j}_1(\mathbf{r})$, which is dominated by the transport current $\mathbf{j}_{\text{tr}}(\mathbf{r}) = (j_+ e^{y/\lambda} + j_- e^{-y/\lambda}) \mathbf{e}_x$. Figure 3(c) shows the normal current density $\mathbf{j}_n(\mathbf{r})$, which is proportional to $\boldsymbol{\varepsilon}(\mathbf{r})$. The supercurrent density $\mathbf{j}_{\text{sl}}(\mathbf{r})$ shown in Fig. 3(d) dominates in the distant region and is depleted in the core region. Figure 4 shows the backflow, which is defined as $\mathbf{j}_1(\mathbf{r}) - \mathbf{j}_{\text{tr}}(\mathbf{r})$, and the magnetic field for backflow $\mathbf{h}_1(\mathbf{r}) - \mathbf{h}_{\text{tr}}(\mathbf{r})$ with $\mathbf{h}_{\text{tr}}(\mathbf{r}) = \mu_0 \lambda (j_+ e^{y/\lambda} - j_- e^{-y/\lambda}) \mathbf{e}_z$ to confirm the validity of our calculations by a comparison with the results of Hu and Thompson (Fig. 2 in Ref. [43]). Our results and the earlier results exhibit similar patterns with a pair of circular currents near the core. We note that the backflow is one order of magnitude smaller than $\mathbf{j}_n(\mathbf{r})$ in the core region. Figure 5 shows the current distribution (arrows) and magnetic field (density plot). Note that we set $v/v_0 = 0.05$ for this figure to emphasize the similarity between this figure and Fig. 1 for a classical fluid.

Figure 6 shows the amplitude of the order parameter. In Fig. 6(a), $f_0(r)$ dominates and thus we extract $f_1(\mathbf{r})$ in Fig. 6(b). We see that $f_1(\mathbf{r})$ is negative in front of the moving vortex ($y < 0$) and positive behind it ($y > 0$). This behavior can be understood on the basis of Eq. (32b) for $f_1(\mathbf{r})$. We can see that

$$f_1(\mathbf{r}) \sim -\frac{\mathbf{j}_0(\mathbf{r}) \cdot \mathbf{j}_{\text{sl}}(\mathbf{r})}{j_c^2} \quad (39)$$

[j_c is defined in Eq. (36d)] when we assume that

$$H_f \sim -\frac{2B_c^2}{\mu_0}, \quad f_v \sim 0, \quad (40)$$

in Eq. (32b). The assumption in Eq. (40) holds for the region farther than ξ from the vortex. In front of the moving vortex ($y < 0$), $\mathbf{j}_0(\mathbf{r})$ and $\mathbf{j}_{\text{sl}}(\mathbf{r})$ are parallel to each other. Behind the moving vortex ($y > 0$), the two current densities are antiparallel to each other [see Figs. 3(a) and 3(d)]. The numerical results shown in Fig. 6 and Eq. (39) are thus consistent. This result is physically reasonable because the local value of the order parameter amplitude should be more suppressed under a larger current density.

B. Local force densities, energy flow, and dissipation function

For the local Lorentz force density and magnetic energy density, we found that the $O(v^2)$ terms are negligible for

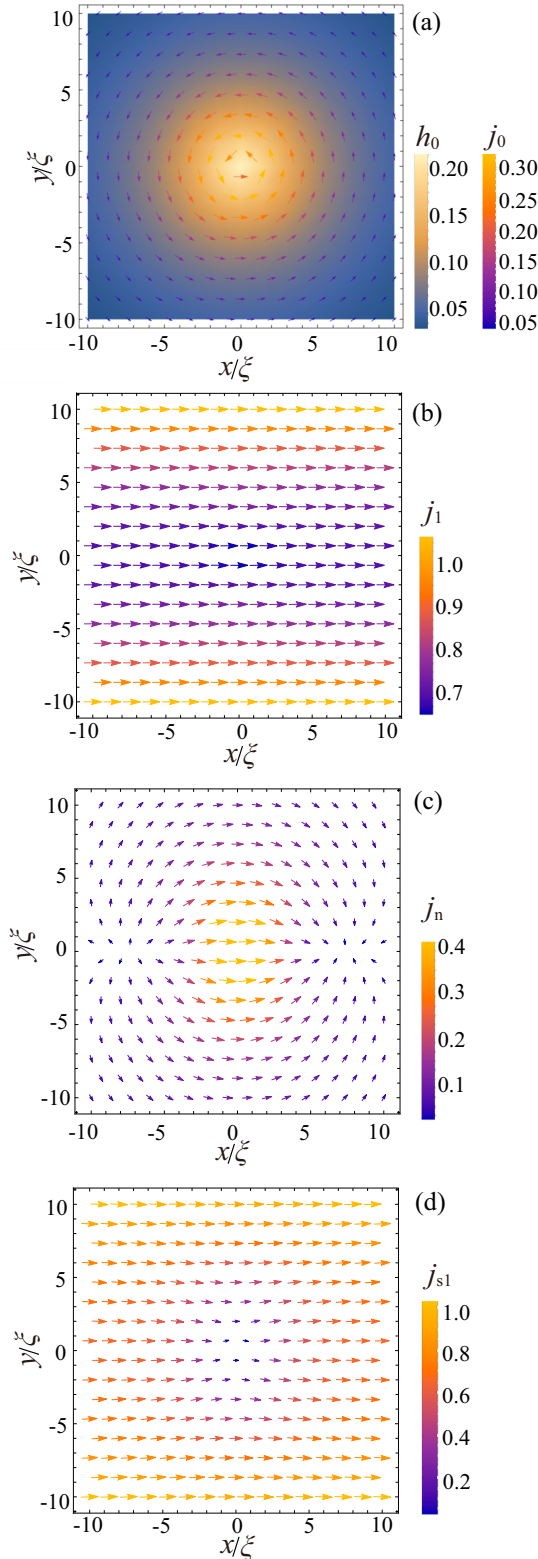


FIG. 3. Current densities and magnetic fields $\kappa = 10$ and $\zeta = 1/3$. (a) $\mathbf{j}_0(\mathbf{r})$ (arrows) with the unit $\frac{\sqrt{2}vB_c}{\mu_0\lambda}$ and $\mathbf{h}_0(\mathbf{r})$ (density) with the unit $\sqrt{2}B_c$. (b) $\mathbf{j}_1(\mathbf{r})$ (arrows) with the unit $\frac{\sqrt{2}vB_c}{\mu_0\lambda v_0}$ and $\mathbf{h}_1(\mathbf{r})$ (density) with the unit $\frac{\sqrt{2}vB_c}{\mu_0\lambda v_0}$. (c) Normal component of the current density $\mathbf{j}_n(\mathbf{r})$ with the unit $\frac{\sqrt{2}vB_c}{\mu_0\lambda v_0}$. This figure can be seen as that for $\boldsymbol{\varepsilon}(\mathbf{r})$ with the unit $2vB_c$. (d) Supercurrent density $\mathbf{j}_{s1}(\mathbf{r})$ with the unit $\frac{\sqrt{2}vB_c}{\mu_0\lambda v_0}$.

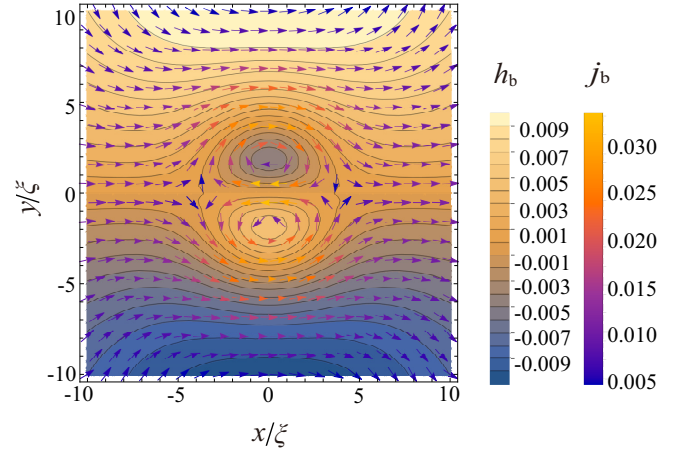


FIG. 4. Backflow $\mathbf{j}_1(\mathbf{r}) - \mathbf{j}_{tr}(\mathbf{r})$ (arrows) and magnetic field $\mathbf{h}_1(\mathbf{r}) - \mathbf{h}_{tr}(\mathbf{r})$ (density plot) for $\kappa = 10$ and $\zeta = 1/3$. Left and right color bars show values for the magnetic field and current density, respectively, in the units $\frac{\sqrt{2}vB_c}{v_0}$ and $\frac{\sqrt{2}vB_c}{\mu_0\lambda v_0}$.

$v/v_0 \leq 0.01$, where the Lorentz force density and magnetic energy density are dominated by the $O(v^0)$ terms $\mathbf{j}_0(\mathbf{r}) \times \mathbf{h}_0(\mathbf{r})$ and $\mathbf{h}_0(\mathbf{r})^2/(2\mu_0)$. The $O(v^0)$ term of the magnetic energy density is axisymmetrically distributed and accordingly the $O(v^0)$ term of the Lorentz force density is oriented in the radial direction.

To examine the net force and net magnetic pressure in the region near the vortex core, we present, in Fig. 7, the local Lorentz force density (arrows) and magnetic pressure (density plot) subtracted by the $O(v^0)$ terms. The local Lorentz force near the core region is oriented downward. The higher magnetic energy density puts more pressure on adjacent regions than does the lower magnetic energy density and thus the net magnetic pressure on the region near the vortex is oriented downward. This agrees with the direction of $\mathbf{j}_{tr}(\mathbf{0}) \times \boldsymbol{\phi}_0$. Figure 8 shows the local hydrodynamic force density $-\partial_\nu \mathcal{P}_{\mu\nu}$, where the force density has the same direction as that of the

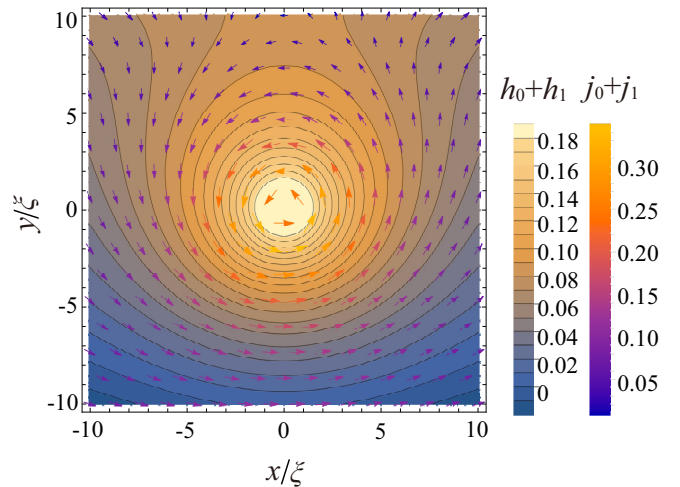


FIG. 5. $\mathbf{j}_0(\mathbf{r}) + \mathbf{j}_1(\mathbf{r})$ (arrow) and $\mathbf{h}_0(\mathbf{r}) + \mathbf{h}_1(\mathbf{r})$ (density plot) for $\kappa = 10$, $\zeta = 1/3$, and $v/v_0 = 0.05$. Left and right color bars show values for the magnetic field and current density, respectively, in the units $\sqrt{2}B_c$ and $\frac{\sqrt{2}vB_c}{\mu_0\lambda}$.

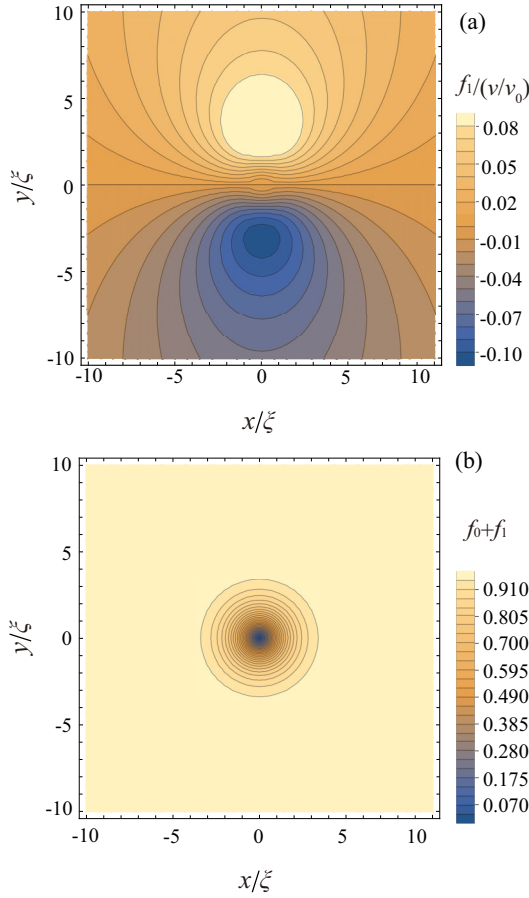


FIG. 6. Amplitude of the order parameter for $\kappa = 10$, $\zeta = 1/3$, and $v/v_0 = 0.003$. (a) $f_1(\mathbf{r})$ in the unit v/v_0 and (b) $f_0(\mathbf{r}) + f_1(\mathbf{r})$.

local Lorentz force density in the region $r \leq 5\xi$ but the magnitude of the local hydrodynamic force density is one order of magnitude larger than that of local magnetic Lorentz force. In the region $r \geq 5\xi$, the two force densities are in opposite

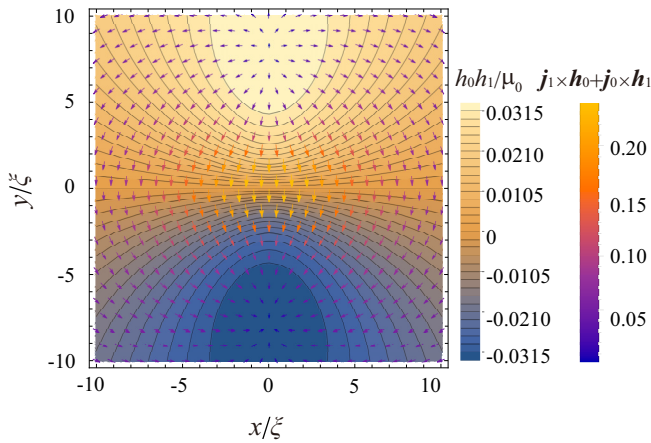


FIG. 7. Local Lorentz force density $[\mathbf{j}_0(\mathbf{r}) + \mathbf{j}_1(\mathbf{r})] \times [\mathbf{h}_0(\mathbf{r}) + \mathbf{h}_1(\mathbf{r})]$ subtracted by $\mathbf{j}_0(\mathbf{r}) \times \mathbf{h}_0(\mathbf{r})$ (arrows) and magnetic energy density $[\mathbf{h}_0(\mathbf{r}) + \mathbf{h}_1(\mathbf{r})]^2 / 2\mu_0$ subtracted by $\mathbf{h}_0(\mathbf{r})^2 / 2\mu_0$ (density plot) for $\kappa = 10$, $\zeta = 1/3$, and $v/v_0 = 0.003$. Left and right color bars show values for the magnetic energy density and local Lorentz force density, respectively, in the units $\frac{B_c^2 v}{\mu_0 v_0}$ and $\frac{c(\kappa)_{\text{IR}} |\phi_0|}{\lambda}$.

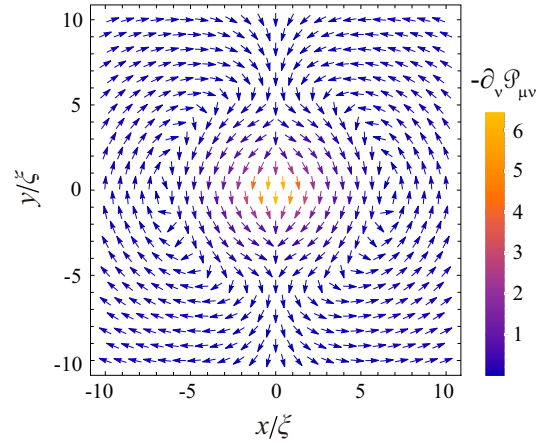


FIG. 8. Local hydrodynamic force density $-\partial_v \mathcal{P}_{\mu\nu}$ for $\kappa = 10$, $\zeta = 1/3$, and $v/v_0 = 0.003$. The unit for intensity is $\frac{c(\kappa)_{\text{IR}} |\phi_0|}{\lambda}$.

directions and practically cancel each other. Figure 9 shows the dissipation function $W(\mathbf{r})$ defined in Eq. (23) (density) and the $O(v^2)$ terms of the energy current density $\mathbf{j}_E(\mathbf{r})$ defined in Eq. (22) (arrows). We see that $\mathbf{j}_E(\mathbf{r})$ is oriented toward the core region and that the dissipation function W is intense in the core region $r < 2\xi$ but is distributed in the region $r \leq \lambda$. In Eq. (23), $\boldsymbol{\varepsilon}_1(\mathbf{r})$, $P_1(\mathbf{r})$, and ∇f_0 are distributed in the regions up to the distance λ , ℓ_P , and ξ , respectively, and thus the dissipation region around the vortex core is given by $r \leq \lambda$.

C. Momentum flow into cylindrical region that contains vortex

We examine the magnitude and path dependence of the magnetic force, $\mathbf{F}_{\text{mag}}(C)$, to determine whether this force can be regarded as the driving force on the vortex and whether it can account for the full magnitude of the driving force.

We take as C a circle whose center is the vortex core and plot the radius R dependence of the magnetic Lorentz force

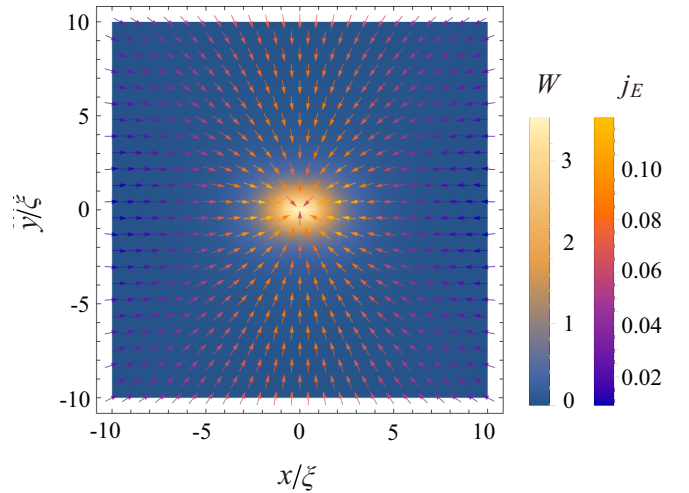


FIG. 9. Dissipation function $W(\mathbf{r})$ defined in Eq. (23) (density) and $O(v^2)$ terms of the energy current density $\mathbf{j}_E(\mathbf{r})$ defined in Eq. (22) (arrows) for $\kappa = 10$, $\zeta = 1/3$, and $v/v_0 = 0.003$. Left color bar shows values for W in the unit $2\sigma_n v^2 B_c^2$ and right one those of $O(v^2)$ terms of $\mathbf{j}_E(\mathbf{r})$ in the unit of $\frac{v^2 B_c^2}{v_0 \mu_0}$.

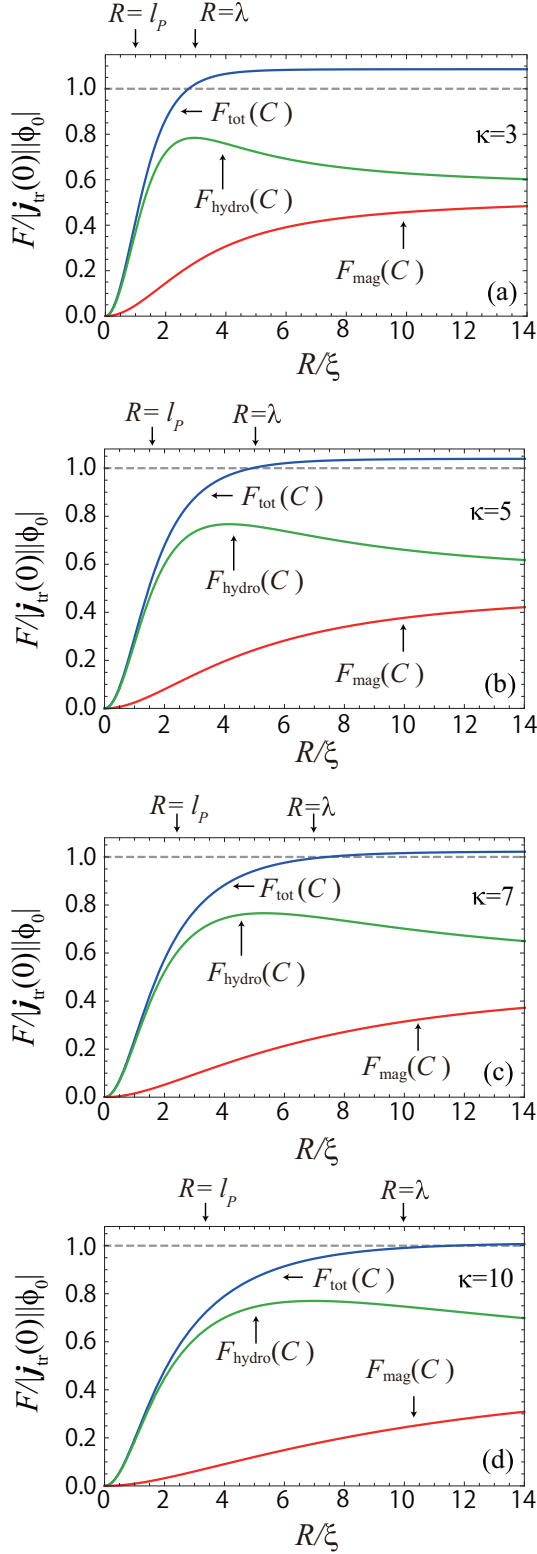


FIG. 10. Radius dependence of the hydrodynamic force $F_{\text{hydro}}(C)$, Eq. (41), magnetic Lorentz force $F_{\text{mag}}(C)$, Eq. (6), and total force $F_{\text{tot}}(C) = F_{\text{hydro}}(C) + F_{\text{mag}}(C)$, Eq. (8), per unit length along the vortex axis for $\zeta = 1/3$ and $\kappa = 3, 5, 7, 10$ [from (a) to (d)]. Horizontal dotted lines indicate $|\mathbf{j}_{\text{tr}}(\mathbf{0})||\boldsymbol{\phi}_0|$.

$F_{\text{mag}}(C)$ acting on the region surrounded by C in Fig. 10. We see that the magnetic force depends on the path and does not

reach half $c(\kappa)|\mathbf{j}_{\text{tr}}(\mathbf{0}) \times \boldsymbol{\phi}_0|$. On this basis, we confirm that the magnetic Lorentz force cannot be regarded as the force on the vortex alone. Let us consider the hydrodynamic force

$$[\mathbf{F}_{\text{hydro}}(C)]_{\mu} = - \oint_C d\ell \mathcal{P}_{\mu\nu} n_{\nu} \quad (41)$$

in a similar way. In Fig. 10, $F_{\text{hydro}}(C)$ depends on R and its magnitude does not reach $c(\kappa)|\mathbf{j}_{\text{tr}}(\mathbf{0}) \times \boldsymbol{\phi}_0|$.

In this figure, we see that the sum of the two forces in Eq. (8) is practically independent of $R \geq \lambda$ for $\kappa = 3, 5, 7, 10$ and thus can be regarded as the force on the vortex core. The magnitude of this force coincides with $c(\kappa)|\mathbf{j}_{\text{tr}}(\mathbf{0}) \times \boldsymbol{\phi}_0|$ for $\kappa = 3, 5, 7, 10$. The effect of the factor $c(\kappa)$ is small for $\kappa = 10$ but is visible for $\kappa = 3, 5, 7$.

It has been claimed that the driving force $\mathbf{j}_{\text{tr}} \times \boldsymbol{\phi}_0$ on the vortex in the London equation is a purely hydrodynamic force (e.g., [17] and [46]). However, in Fig. 10, even for $\kappa = 10$ (which is a relatively large value), the driving force is not purely hydrodynamic around $R \geq \lambda$, where the driving force becomes R -independent.

We also note that the magnitude of the magnetic Lorentz force is less than half $|\mathbf{j}_{\text{tr}}(\mathbf{0}) \times \boldsymbol{\phi}_0|$ for an arbitrary value of R . This result can be indirectly tested experimentally, as discussed in Sec. V D.

V. EXTENSION BASED ON VARIANTS OF CONVENTIONAL TDGL EQUATION

We discuss the applicability of our conclusion on the driving force to other types of TDGL equations in Secs. V A and V B. We then discuss the implication on the multiple-vortex state and the pinned vortex in Sec. V C. The force on a segment of a curved vortex line is discussed in Appendix A.

A. Validity of results for conventional TDGL equation

The TDGL equation, shown in Eqs. (16a) and (16b), is valid only when the pair-breaking mean free time is much smaller than $\hbar/\Delta(T)$ near T_c [$\Delta(T)$ is the energy gap for the excitation in the uniform state]. The region of validity of the TDGL is small. Here, we demonstrate that our main assertion regarding the driving force on the vortex holds in the generalized TDGL equation derived by Watts-Tobin, Krähenbühl, and Kramer [47].

When the mean-free time due to nonmagnetic impurities τ_{imp} is much smaller than $\hbar/\Delta(T)$ but the spin-flip relaxation time τ_{sf} or inelastic mean-free time τ_E is larger than $\hbar/\Delta(T)$, the conventional TDGL equation [Eqs. (16a) and (16b)] is replaced by the following set of equations (generalized TDGL equation):

$$\gamma^{(f)} \frac{\partial f}{\partial t} = \xi^2 \nabla^2 f - \left(\frac{e^* \xi \mathbf{Q}}{\hbar} \right)^2 f + f - f^3, \quad (42a)$$

$$\nabla \cdot \mathbf{j}_s = \frac{\gamma^{(x)} f^2 P}{\mu_0 \lambda^2 \xi^2}, \quad (42b)$$

with

$$\begin{aligned} \gamma^{(f)} &= \gamma [1 + 4\tau_E^2 \Delta(T)^2 f^2 / \hbar^2]^{\frac{1}{2}}, \\ \gamma^{(x)} &= \gamma [1 + 4\tau_E^2 \Delta(T)^2 f^2 / \hbar^2]^{-\frac{1}{2}}. \end{aligned} \quad (43)$$

Here we assume that $\tau_{sf} \gg \tau_E$. The symbols $\gamma^{(f)}$ and $\gamma^{(x)}$, respectively, represent the relaxation times for the amplitude and phase of the order parameter. When $\tau_E \Delta(T)/\hbar \ll 1$, $\gamma^{(f)} \sim \gamma^{(x)}$, and Eqs. (42a) and (42b) reduce to the conventional TDGL equation [Eqs. (16a) and (16b)].

Correspondingly, the momentum balance relation Eq. (25) for the conventional TDGL equation is replaced by

$$\begin{aligned} \partial_v(-\mathcal{P}_{\mu\nu} + T_{\mu\nu}) + \tilde{\gamma}^{(f)} \partial_\mu f \partial_t f \\ - \tilde{\gamma}^{(x)} (2\pi/|\phi_0|)^2 f^2 P Q_\mu - (\mathbf{j}_n \times \mathbf{h})_\mu \\ = 0. \end{aligned} \quad (44)$$

In the dissipation-free region, $\partial_t f \sim 0$, $P \sim 0$, $\mathbf{j}_n \sim 0$, and Eq. (44) reduces to Eq. (7), from which the path independence of the total force Eq. (8) follows and the driving force on the vortex becomes well defined.

B. TDGL equation allowing for Hall effect

In the conventional TDGL equation and the generalized TDGL equation in the previous subsection, the vortex flows perpendicular to the magnetic field and transport current; i.e., the Hall effect cannot be described. The conventional TDGL equation has been generalized so that the Hall effect can be discussed by introducing a complex relaxation time $\gamma \rightarrow \gamma + i\gamma'$. The flux flow Hall conductivity was discussed with this variant of the TDGL equation in [35,36]. In this subsection, we discuss how the momentum balance relation and the force on the vortex are modified in this variant of the TDGL equation and show that our results on the driving force still hold.

In this variant of the TDGL equation, Eqs. (16a) and (16b) are respectively modified as

$$\gamma \frac{\partial f}{\partial t} - \gamma' \frac{e^* P f}{\hbar} = \xi^2 \nabla^2 f - \left(\frac{e^* \xi \mathbf{Q}}{\hbar} \right)^2 f + f - f^3 \quad (45)$$

and

$$\frac{\partial \rho_s}{\partial t} + \nabla \cdot \mathbf{j}_s = \tilde{\gamma} \left(\frac{2\pi}{|\phi_0|} \right)^2 f^2 P, \quad \rho_s := -\frac{\gamma' \hbar f^2}{2\mu_0 e^* \lambda^2 \xi^2}. \quad (46)$$

Here, the new terms are underlined (all new terms are underlined in this subsection). The momentum balance relation Eq. (25) is then modified as

$$\begin{aligned} \partial_t(-\rho_s Q_\mu) + \partial_v \left(\mathcal{P}'_{\mu\nu} - \mathcal{T}_{\mu\nu} \right) \\ = \rho_s \mathbf{e}_\mu + \tilde{\gamma} \partial_\mu f \partial_t f - \tilde{\gamma} \left(\frac{2\pi}{|\phi_0|} \right)^2 f^2 P Q_\mu - (\mathbf{j}_n \times \mathbf{h})_\mu, \end{aligned} \quad (47)$$

with

$$\mathcal{P}'_{\mu\nu} = \mathcal{P}_{\mu\nu} - \delta_{\mu\nu} \rho_s P. \quad (48)$$

We see that Eq. (47) is reduced to Eq. (25) when $\rho_s = 0$. Equation (47) consists of the stock term (first term on the left-hand side), flow term (second term on the left-hand side), and sink (right-hand side) of the momentum density. The flow term and sink, respectively, correspond to the driving

force and the environmental force. There is no consensus on whether the stock term should be assigned to the driving force or the environmental force. We remark that the driving force obtained from this variant of the TDGL equation is the same as that obtained in the conventional TDGL equation. The additional term $(-\rho_s P)$ in the momentum flux tensor does not contribute to the driving force, because P practically vanishes in the dissipation-free region.

Rewriting Eq. (47) and integrating both sides yield the force balance relation

$$\begin{aligned} c(\kappa) \mathbf{j}_r(\mathbf{0}) \times \phi_0 = \tilde{\gamma} \int d\mathbf{r} (\nabla f f_v + \underline{(2\pi/|\phi_0|)^2 f^2 P Q_0}) \\ + \int d\mathbf{r} \mathbf{j}_n \times \mathbf{h}, - \int d\mathbf{r} (\underline{Q_0 \partial_t \rho_s} - \underline{P \nabla \rho_s}), \end{aligned} \quad (49)$$

which reduces to Eq. (34) when we set $\rho_s = 0$ ($\tilde{\gamma}' = 0$). The three underlined terms contribute to the η_2 term in Eq. (4). The second term on the right-hand side on the first line does not depend on ρ_s or $\tilde{\gamma}'$; however, the equation used to solve P contains ρ_s and thus P is modified so that it contributes to the η_2 term. The η_2 term in the environmental force Eq. (4) is responsible for the Hall effect. At the early stage of some discussion of the Hall effect in superconductors, this term was introduced in [46,48] as a Magnus-type force with a reduced amplitude. The authors of [48] did not show the origin of this force. We thus emphasize that the force $\eta_2 \mathbf{e}_z \times \mathbf{v}$ does not originate from momentum transfer from the distant region (dissipation-free region) to the core region.

C. Driving force on pinned vortex, size of core region, and multiple vortices

The present scheme is applicable for deriving the driving force on a vortex pinned by a columnar defect parallel to the z axis. For such a vortex, the TDGL equation [Eqs. (16a) and (16b)] is replaced by the static Ginzburg-Landau equation

$$U(r) f = \xi^2 \nabla^2 f - \left(\frac{e^* \xi \mathbf{Q}}{\hbar} \right)^2 f + f - f^3, \quad (50a)$$

$$\nabla \cdot f^2 \mathbf{Q} = 0. \quad (50b)$$

Here, $U(r)$ denotes a uniform pinning potential along the z axis. From Eqs. (50a), (50b), and the Ampère law Eq. (17), the momentum balance relation for the pinned vortex is

$$\partial_v (T_{\mu\nu} - \mathcal{P}_{\mu\nu}) + U(\mathbf{r}) f \partial_\mu f = 0. \quad (51)$$

We see that the relation $\partial_v (T_{\mu\nu} - \mathcal{P}_{\mu\nu}) = 0$ holds in the region where the pinning potential is zero. We refer to this region as the pinning-free region. It follows that the sum of the hydrodynamic force and the magnetic force acting on the region surrounded by the closed loop C does not depend on the

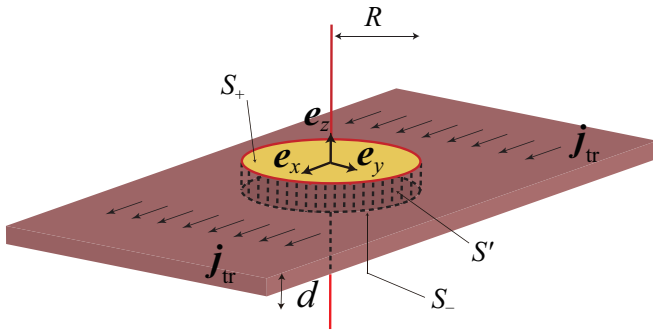


FIG. 11. Setup for calculation of the force on the Pearl vortex in a 2D superconductor. The transport magnetic field in the z direction is perpendicular to the wide surface of the slab. The transport current flows uniformly in the x direction and varies along the y axis. The closed surface S consists of the surface S_+ , bottom S_- , and side S' . The normal vector S points outward.

choice of C but depends on the winding number of C around the vortex center. Under the same boundary condition as that for the flow state, the path-independent driving force on the pinned vortex is given by $c(\kappa)\mathbf{j}_{\text{tr}}(\mathbf{0}) \times \boldsymbol{\phi}_0$.

A crucial difference between flowing and pinned vortices is the different conditions required for the driving force on the vortex to be well defined. We saw in Fig. 10 that the path-independent force is realized when the radius R is larger than λ . For the pinned vortex, the path-independent force can be defined when the radius R is larger than the range of the pinning potential. This implies that the (path-independent) driving force on the flowing vortex lattice can be defined only when the intervortex distance is larger than λ ; this condition is realized in the external field near the lower critical field H_{c1} . In contrast, the (path-independent) driving force on the pinned vortex lattice is well defined when the intervortex distance is larger than the range of the pinning potential. When the range of the pinning potential is on the order of ξ or smaller, this condition is realized practically in all field ranges of the magnetic field lower than the upper critical field H_{c2} .

VI. FORCE ON PEARL VORTEX

This paper mostly focuses on the force on a vortex in three-dimensional (3D) superconductors (with a demagnetization factor of zero). Quantum vortices also play an important role in 2D superconductors. We thus consider the driving force on a pinned vortex in 2D superconductors, namely the Pearl vortex, with the London equation for the outside of the core region within a distance of $r_c = O(\xi)$ from the vortex. At the end of this section, we briefly discuss the driving force on a flowing Pearl vortex.

We consider a superconductor with a slab thickness d that is much smaller than λ . The areal dimension of the slab is taken to be infinite. We set the normal direction of the slab to be along the z axis. We express the position vector in 3D space as $\mathbf{r} = \mathbf{r}_\perp + z\mathbf{e}_z$ with $\mathbf{r}_\perp \cdot \mathbf{e}_z = 0$. We consider that the current density is uniform along the z direction for $|z| < d/2$ (see Fig. 11). We can obtain the vector potential via the Maxwell-

London equation [38]

$$\nabla^2 \mathbf{A} = -\mu_0 \mathbf{j}_s = \frac{2\delta(z)}{\lambda_{\text{eff}}} (-\boldsymbol{\Phi} + \mathbf{A}), \quad (52)$$

$$\boldsymbol{\Phi} = \frac{\hbar}{e^* r_\perp} \mathbf{e}_\theta = \frac{\hbar}{e^*} \mathbf{e}_z \times \frac{\mathbf{r}_\perp}{r_\perp}, \quad (53)$$

with the effective penetration depth $\lambda_{\text{eff}} = 2\lambda^2/d$ in 2D superconductors [38]. We assume that $r_c \ll \lambda_{\text{eff}}$. The momentum flow in the core region is $O((r_c/\lambda_{\text{eff}})^2)$. It is thus ignored in the following. We seek the solution to Eq. (52) in the presence of a transport current. We derive the magnetic field $\mathbf{h}(r_\perp, z)$ and the current density $\mathbf{j}(r_\perp, z)$ from the vector potential, with which we can calculate the inward flow of hydrodynamic momentum into the region V through the surface $S (= \partial V)$,

$$[\mathbf{F}_{\text{hydro}}(S)]_\mu = - \oint_S dS \mathcal{P}_{\mu\nu} n_\nu, \quad (54)$$

with Eq. (27) and the inward flow of magnetic momentum into the region V through the surface S ,

$$[\mathbf{F}_{\text{mag}}(S)]_\mu = \oint_S dS \mathcal{T}_{\mu\nu} n_\nu, \quad \mathcal{T}_{\mu\nu} = \frac{1}{\mu_0} \left(h_\mu h_\nu - \frac{\delta_{\mu\nu}}{2} \mathbf{h}^2 \right). \quad (55)$$

It follows that for $V \subset V'$,

$$\begin{aligned} & \mathbf{F}_{\text{hydro}}(S = \partial V)_\mu + \mathbf{F}_{\text{mag}}(S = \partial V)_\mu \\ &= \mathbf{F}_{\text{hydro}}(S' = \partial V')_\mu + \mathbf{F}_{\text{mag}}(S' = \partial V')_\mu, \end{aligned} \quad (56)$$

from the relations $\partial_\nu P_{\mu\nu} = (\mathbf{j} \times \mathbf{h})_\mu$ and $\partial_\nu T_{\mu\nu} = (\mathbf{j} \times \mathbf{h})_\mu$, which hold in the London and Maxwell equations, respectively. When we take V to be the core region (i.e., $\mathbf{r}_\perp \sim 0$ and $z \sim 0$), the sum of the two forces $\mathbf{F}_{\text{hydro}}(S')$ and $\mathbf{F}_{\text{mag}}(S')$ does not depend on the choice of V' so long as $V \subset V'$ is satisfied. Thus, the sum of the two forces is not exerted on the region $V' - V$; it is only exerted on the core region V . In 2D superconductors, the driving force on a vortex consists of the hydrodynamic force and the magnetic Lorentz force, as is the case for 3D superconductors.

It is important to determine how much $\mathbf{F}_{\text{hydro}}(S)$ or $\mathbf{F}_{\text{mag}}(S)$ contributes to the driving force on the vortex in 2D superconductors. We consider this issue more explicitly below. Our goal is to derive the expressions for the hydrodynamic force Eq. (78) and the magnetic force (79), which are shown in Fig. 12, and discuss their implications.

The solution to Eq. (52) in the presence of a transport current is given by the sum of $\mathbf{A}_{\text{tr}}(r_\perp, z)$ and $\mathbf{A}_{\text{Pearl}}(r_\perp, z)$. Here, $\mathbf{A}_{\text{tr}}(r_\perp, z)$ is a solution to the homogeneous equation

$$\nabla^2 \mathbf{A} + \frac{2\delta(z)}{\lambda_{\text{eff}}} \mathbf{A} = 0 \quad (58)$$

that describes the transport current without a vortex. $\mathbf{A}_{\text{Pearl}}(r_\perp, z)$ is the solution to Eq. (52) in the absence of a transport current.

We see that

$$\mathbf{A}_{\text{tr}}(r_\perp, z) = A_1 \left(1 + \frac{|z|}{2\lambda_{\text{eff}}} \right) \mathbf{e}_x \quad (59)$$

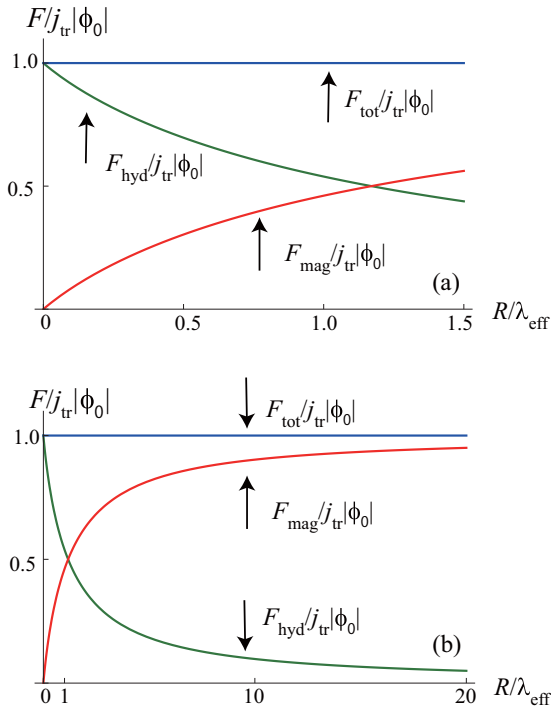


FIG. 12. Force on Pearl vortex in a 2D superconductor with thickness d that is much smaller than the penetration depth λ . Calculation is based on the Maxwell-London equation Eq. (52), namely the radial dependence of the hydrodynamic force Eq. (54) and the magnetic force Eq. (55) on the vortex in the presence of the transport current j_{tr} . The characteristic scale $\lambda_{\text{eff}} = 2\lambda^2/d$ is the effective magnetic screening length in the 2D superconductor. The top panel (a) shows the spatial range on the order of $R \sim \lambda_{\text{eff}}$ and the bottom panel (b) shows the results in a much wider range of R .

is one of the solutions to Eq. (58). From Eq. (59), the magnetic field

$$\mathbf{h}_{\text{tr}}(\mathbf{r}_{\perp}, z) = \nabla \times \mathbf{A}_{\text{tr}}(\mathbf{r}_{\perp}, z) = \frac{A_1 \text{sgn}(z)}{2\lambda_{\text{eff}}} \mathbf{e}_y \quad (60)$$

and the current density

$$\mathbf{j}_{\text{tr}}(\mathbf{r}_{\perp}, z) = \frac{1}{\mu_0} \nabla \times \mathbf{h}_{\text{tr}}(\mathbf{r}_{\perp}, z) = -\mathbf{e}_x \frac{A_1}{\mu_0 \lambda_{\text{eff}}} \delta(z) \quad (61)$$

follow. Equation (61) shows that the solution Eq. (59) describes the transport current in the absence of a vortex. For later convenience, we introduce the notation $j_{\text{tr}} = -A_1/(\mu_0 \lambda_{\text{eff}} d)$ and respectively write Eqs. (60) and (61) as

$$\mathbf{h}_{\text{tr}}(\mathbf{r}_{\perp}, z) = -\frac{\mu_0 j_{\text{tr}} d}{2} \text{sgn}(z) \mathbf{e}_y, \quad \mathbf{j}_{\text{tr}}(\mathbf{r}_{\perp}, z) = j_{\text{tr}} d \delta(z) \mathbf{e}_x. \quad (62)$$

The Pearl solution (isolated vortex in the absence of a transport current) is given by

$$\mathbf{A}_{\text{Pearl}}(\mathbf{r}_{\perp}, z) = \mathbf{e}_{\theta} A(r_{\perp}, z) \quad (63)$$

with

$$A(r_{\perp}, z) = |\phi_0| \int_0^{\infty} \frac{dq_{\perp}}{2\pi} \frac{e^{-q_{\perp}|z|} J_1(q_{\perp} r_{\perp})}{(1 + \lambda_{\text{eff}} q_{\perp})}. \quad (64)$$

From Eqs. (63) and (64), we can derive the magnetic field $\mathbf{h}_{\text{Pearl}}(\mathbf{r}_{\perp}, z) = h_{r_{\perp}}(\mathbf{r}_{\perp}, z) \mathbf{e}_{r_{\perp}} + h_z(\mathbf{r}_{\perp}, z) \mathbf{e}_z = \nabla \times \mathbf{A}_{\text{Pearl}}$ and the current density \mathbf{j} , as shown in Appendix B.

The physical quantities necessary to calculate the driving force on a vortex are listed below. The current density is given by

$$\mathbf{j}_{\text{Pearl}}(\mathbf{r}_{\perp}, z) = \delta(z) \mathbf{e}_{\theta} j_{2D}(r_{\perp}), \quad (65)$$

$$j_{2D}(r_{\perp}) = \frac{|\phi_0|}{\pi \mu_0 \lambda_{\text{eff}}^2} \left[\frac{\lambda_{\text{eff}}}{r_{\perp}} - \vartheta\left(\frac{r_{\perp}}{\lambda_{\text{eff}}}\right) \right], \quad (66)$$

with

$$\int_0^{\infty} \frac{J_1(sx)}{1+s} ds = \frac{\pi}{2} \left[H_{-1}(x) - N_{-1}(x) + \frac{2}{\pi x} \right] \equiv \vartheta(x), \quad (67)$$

where $J_n(x)$, $H_n(x)$, and $N_n(x)$ respectively denote the n th-order Bessel function, n th-order Struve function of the first kind, and n th-order Neumann function. The radial and z components of the magnetic field near $z = 0$ are given by

$$h_r(\mathbf{r}_{\perp}, z \rightarrow \pm 0) = \pm \frac{|\phi_0|}{2\pi \lambda_{\text{eff}}^2} \left[\frac{\lambda_{\text{eff}}}{r_{\perp}} - \vartheta\left(\frac{r_{\perp}}{\lambda_{\text{eff}}}\right) \right], \quad (68)$$

$$h_z(\mathbf{r}_{\perp}, 0) = \frac{|\phi_0|}{2\pi \lambda_{\text{eff}}^2} \varpi\left(\frac{r_{\perp}}{\lambda_{\text{eff}}}\right), \quad (69)$$

with

$$\varpi(x) \equiv \frac{1}{x} \frac{d}{dx} [x \vartheta(x)] \quad (70)$$

$$= \frac{1}{x} + \frac{\pi}{2} [-H_0(x) + N_0(x)], \quad (71)$$

as derived in Appendix B.

We are now ready to calculate the force on the vortex. We take the region V that contains the vortex as

$$V = \{(\mathbf{r}_{\perp}, z) | r_{\perp} \leq R, \quad |z| \leq d/2\} \quad (72)$$

and decompose the surface S of V as

$$S = S_+ \cup S_- \cup S', \quad (73)$$

with

$$S_{\pm} = \{(\mathbf{r}_{\perp}, z) | r_{\perp} \leq R, \quad z = \pm d/2\}, \quad (74)$$

$$S' = \{(\mathbf{r}_{\perp}, z) | r_{\perp} = R, \quad |z| \leq d/2\} \quad (75)$$

(see Fig. 11). The normal vectors are $\mathbf{n} = \pm \mathbf{e}_z$ on S_{\pm} and $\mathbf{n} = \mathbf{e}_{r_{\perp}}$ on S' . For the hydrodynamic force Eq. (54), the surfaces S_{\pm} do not contribute and thus

$$[\mathbf{F}_{\text{hydro}}(S)]_{\mu} = - \int_{S'} dS \mathcal{P}_{\mu\nu} n_{\nu}. \quad (76)$$

In the integral over S' , we replace the expressions for the current densities in Eqs. (62) and (65) with

$$\mathbf{j}_{\text{tr}}(\mathbf{r}_{\perp}, z) = j_{\text{tr}} \mathbf{e}_x \Theta\left(\frac{d}{2} - |z|\right), \quad (77a)$$

$$\mathbf{j}_{\text{Pearl}}(\mathbf{r}_{\perp}, z) = \mathbf{e}_{\theta} j_{2D}(r_{\perp}) \Theta\left(\frac{d}{2} - |z|\right), \quad (77b)$$

with the Heaviside's step function $\Theta(x) = 1$ for $x > 0$ and 0 otherwise. Substituting Eqs. (77a) and (77b) into $\mathcal{P}_{\mu\nu}$ in Eq. (76) yields

$$\mathbf{F}_{\text{hydro}}(S) = -e_y j_{\text{tr}} |\phi_0| d \left[1 - \frac{R}{\lambda_{\text{eff}}} \vartheta \left(\frac{R}{\lambda_{\text{eff}}} \right) \right]. \quad (78)$$

For $\mathbf{F}_{\text{mag}}(S)$, the contribution from S' is $O(d^2)$ and thus negligible. The contributions from S_+ and S_- are equal. Substituting $\mathbf{h}(\mathbf{r}_\perp, z = +0) = \mathbf{h}_{\text{tr}}(\mathbf{r}_\perp, z = +0) + \mathbf{h}_{\text{Pearl}}(\mathbf{r}_\perp, z = +0)$ with the expressions for magnetic fields in Eqs. (69) and (62) into Eq. (55) yields

$$\mathbf{F}_{\text{mag}}(S) = -e_y j_{\text{tr}} |\phi_0| d \frac{R}{\lambda_{\text{eff}}} \vartheta \left(\frac{R}{\lambda_{\text{eff}}} \right). \quad (79)$$

From Eqs. (78) and (79), we confirm that both $\mathbf{F}_{\text{hydro}}(S)$ and $\mathbf{F}_{\text{mag}}(S)$ depend on the radius R but the sum of the two forces

$$\mathbf{F}_{\text{tot}}(S) = \mathbf{F}_{\text{hydro}}(S) + \mathbf{F}_{\text{mag}}(S) = -e_y j_{\text{tr}} |\phi_0| d \quad (80)$$

does not depend on R . This observation demonstrates that only the sum of the two forces can be regarded as the force on the vortex. Figure 12 shows the radial dependence of $|\mathbf{F}_{\text{tot}}(S)|$, $|\mathbf{F}_{\text{hydro}}(S)|$, and $|\mathbf{F}_{\text{mag}}(S)|$. The asymptotic behavior of $|\mathbf{F}_{\text{hydro}}(S)|$ is given by

$$\frac{|\mathbf{F}_{\text{hydro}}(S)|}{j_{\text{tr}} |\phi_0| d} \sim \begin{cases} 1 - \frac{R}{\lambda_{\text{eff}}}, & \text{for } R \ll \lambda_{\text{eff}}, \\ \frac{\lambda_{\text{eff}}}{R}, & \text{for } \lambda_{\text{eff}} \ll R, \end{cases} \quad (81)$$

and

$$\frac{|\mathbf{F}_{\text{mag}}(S)|}{j_{\text{tr}} |\phi_0| d} \sim \begin{cases} \frac{R}{\lambda_{\text{eff}}}, & \text{for } R \ll \lambda_{\text{eff}}, \\ 1 - \frac{\lambda_{\text{eff}}}{R}, & \text{for } \lambda_{\text{eff}} \ll R, \end{cases} \quad (82)$$

from that of $\vartheta(x)$,

$$\vartheta(x) \sim \begin{cases} 1 + \frac{x}{2} \ln \left(\frac{x e^{x-1/2}}{2} \right) + O(x^2), & \text{for } 0 < x \ll 1, \\ \frac{1}{x} + O(x^{-2}), & \text{for } 1 \ll x. \end{cases} \quad (83)$$

We note that $|\mathbf{F}_{\text{hydro}}(S)|$ dominates $|\mathbf{F}_{\text{mag}}(S)|$ for $R \ll \lambda_{\text{eff}}$ and $|\mathbf{F}_{\text{mag}}(S)|$ dominates $|\mathbf{F}_{\text{hydro}}(S)|$ for $R \gg \lambda_{\text{eff}}$. This is in contrast to the 3D case, where $|\mathbf{F}_{\text{hydro}}(C)|$ is larger than $|\mathbf{F}_{\text{mag}}(C)|$ for all ranges of R and the magnitudes of the two forces approach each other for large R .

The difference from the 3D case stems from (i) the transport current being uniform and (ii) the superconductor being 2D while the magnetic field exists both outside and inside the superconductor.

The radial dependence of the driving force on the Pearl vortex can be understood on the basis of the asymptotic behavior of the current density and magnetic field:

$$j_{2D}(\mathbf{r}_\perp) \sim \begin{cases} \frac{|\phi_0|}{\pi \mu_0 \lambda_{\text{eff}} r_\perp}, & \xi \ll r_\perp \ll \lambda_{\text{eff}}, \\ \frac{|\phi_0|}{\pi \mu_0 r_\perp^2}, & \lambda_{\text{eff}} \ll r_\perp, \end{cases} \quad (84)$$

$$h_z(\mathbf{r}_\perp, 0) \sim \begin{cases} \frac{|\phi_0|}{2\pi \lambda_{\text{eff}} r_\perp}, & \xi \ll r_\perp \ll \lambda_{\text{eff}}, \\ \frac{|\phi_0| \lambda_{\text{eff}}}{\pi r_\perp^3}, & \lambda_{\text{eff}} \ll r_\perp, \end{cases} \quad (85)$$

$$h_r(\mathbf{r}_\perp, z \rightarrow \pm 0) \sim \begin{cases} \pm \frac{|\phi_0|}{2\pi \lambda_{\text{eff}} r_\perp}, & \xi \ll r_\perp \ll \lambda_{\text{eff}}, \\ \pm \frac{|\phi_0|}{2\pi r_\perp^2}, & \lambda_{\text{eff}} \ll r_\perp. \end{cases} \quad (86)$$

Equations (84) and (86) follow from Eq. (83). Equation (85) follows from

$$\varpi(x) \sim \begin{cases} \frac{1}{x} + \ln \left(\frac{x e^x}{2} \right) + O(x), & \text{for } 0 < x \ll 1, \\ \frac{2}{x^3} + O(x^{-5}), & \text{for } 1 \ll x. \end{cases} \quad (87)$$

First, consider the case $R \ll \lambda_{\text{eff}}$. The transport current is uniform and the current density Eq. (84) has the same form as that for the 3D case at short distance $R \ll \lambda$. The z component of the magnetic field Eq. (86) has the same r_\perp dependence as Eq. (84) for $R \ll \lambda_{\text{eff}}$. However, $h_z(\mathbf{r}_\perp, z)$ contributes to the force through S_\pm . Integration over the disk region S_\pm gives the additional factor R , which makes the magnetic contribution small compared to the hydrodynamic contribution through S' .

Next, consider the case $R \gg \lambda_{\text{eff}}$, where the current density Eq. (84) decays faster than $1/r_\perp$ owing to the screening effect. The transport current is uniform and thus the hydrodynamic contribution diminishes at large distance $R \gg \lambda_{\text{eff}}$. This is in marked contrast to the 3D case, where the exponential decay of the circular current density is compensated by the exponential spatial dependence of the transport current density. Consequently, the hydrodynamic contribution to the force on the vortex remains even at large distance $R \gg \lambda$ in the 3D case.

The lost hydrodynamic contribution is compensated by the magnetic contribution through S_\pm . At a larger distance, the integral over the disk region gives a larger contribution than that over the side surface S' . Thus, the difference in the spatial dimensionality in superconductors (2D) and the magnetic field distribution (3D) also accounts for the different radial dependence of the driving force on a vortex in the 2D and 3D cases.

In this section, we have discussed the driving force on the pinned Pearl vortex. For the flowing Pearl vortex, the size of the core region (where dissipation occurs) r_c is on the order of λ_{eff} . In this case, the magnetic contribution to the momentum flow through the surface and the bottom,

$$S_\pm(r_c) = \{[\mathbf{r}_\perp, z | r_\perp \leq r_c, z = \pm d/2], \quad (88)$$

is not negligible. These surfaces belong to the core region, where the London equation is not valid. Thus, the derivation of the driving force on the flowing Pearl vortex requires consideration beyond the London equation. This situation is similar to that for the flowing deformed vortex in 3D superconductors discussed in Appendix A.

VII. DISCUSSION

We first discuss the underlying relation between the driving force and the topological number of vortices in Sec. VII A. We also remark on the Berry phase approach. In Sec. VII B, we propose an experiment that shows that the magnetic Lorentz force does not have the full amplitude expected as the driving force on vortices. In Sec. VII C, we discuss future theoretical issues.

A. Relation between driving force and topological number of quantum vortices

We discuss the underlying physics of the driving force on a vortex in superconductors via a comparison with neutral

superfluids. In neutral superfluids, the circulation is quantized around a quantum vortex,

$$\oint_C d\boldsymbol{\ell} \cdot \mathbf{v}_s(\mathbf{r}) = \pm \frac{2\pi\hbar}{m}, \quad (89)$$

where $\mathbf{v}_s(\mathbf{r})$ is the superfluid velocity and m is of mass of particles. This relation leads to

$$\nabla \times \mathbf{v}_s(\mathbf{r}) = 0 \quad (90)$$

in the dissipation-free region. It follows from Eq. (90) that the momentum flux tensor $\mathcal{P}_{\mu\nu}$ is divergence-free and that the integral of $\mathcal{P}_{\mu\nu}$ Eq. (5) is path-independent and thus eligible as a force on the vortex.

In superconductors, instead of the circulation Eq. (89), London's fluxoid [39] is quantized,

$$\int dS \cdot \mathbf{h}(\mathbf{r}) + \mu_0\lambda \oint_{C(=\partial S)} d\boldsymbol{\ell} \cdot \mathbf{j}_s(\mathbf{r}) = \pm|\phi_0|, \quad (91)$$

when C belongs to the stress-free region. This relation leads to the London equation

$$\nabla \times \mathbf{j}(\mathbf{r}) = \frac{\mathbf{h}(\mathbf{r})}{\mu_0\lambda^2} \quad (92)$$

in the stress-free region. It then follows from Eq. (92) that neither $\mathcal{T}_{\mu\nu}$ nor $\mathcal{P}_{\mu\nu}$ but rather the combination $\mathcal{T}_{\mu\nu} - \mathcal{P}_{\mu\nu}$ is divergence-free and that the integral of the sum of the two tensors is path-independent and thus eligible as a force on the vortex. We can see that different driving forces on the vortices in the two systems result from different quantum numbers that characterize the quantum vortices [Eqs. (89) and (91)] or the different local relations [Eqs. (90) and (92)].

This observation leads us to conclude that the nature of the driving force on quantum vortices is nontrivial in superfluids (superconductors) where the irrotational condition (London equation) is modified. One of the examples is the Mermin-Ho vortex in the A phase of the superfluid ^3He [49], where the irrotational condition Eq. (90) does not hold. We will discuss the driving force on these vortices and related topological objects in superfluids and superconductors in a separate paper.

So far we have discussed the driving force on quantum vortices based on the TDGL equation and its variants for rectilinear vortices in 3D superconductors (Sec. V) and the London equation for the Pearl vortex (Sec. VI) and a curved vortex (Appendix A). In the approach of Ao and Thouless [17], the force

$$2\pi\hbar n_s(\mathbf{v}_s - \mathbf{v}_v) \times \mathbf{e}_z \quad (93)$$

on a vortex toward the z axis was derived with use of the Berry phase, which is the phase that a many-body wave function acquires after an adiabatic motion of a vortex. Here, n_s , \mathbf{v}_s , and \mathbf{v}_v respectively denote the superfluid density, superfluid velocity, and vortex velocity.

The Berry phase approach is valid at zero temperature, whereas the TDGL equation is valid near the transition temperature. The two approaches are thus complementary. In Eq. (93), the term proportional to \mathbf{v}_s corresponds to the driving force in our definition, becoming the same [up to the multiplicative factor $c(\kappa)$] as the driving force in our results if \mathbf{v}_s is properly defined and the effect of the superfluid velocity by the vortex [$\mathcal{Q}_0(\mathbf{r})$ in the notation of the present paper] is taken

into account in the Berry phase calculation. The multiplicative factor $c(\kappa)$ implies that the force derived by the Berry phase approach is not a purely hydrodynamic force.

B. Proposed experiment

It is possible to experimentally test some of our theoretical results if the local magnetic field and the local current density can be measured experimentally (e.g., via SQUID microscopy [50,51]) in the following way:

(1) Allow an external current to flow through a superconductor without a vortex. Measure the spatial current density $\mathbf{j}_{\text{tr}}(\mathbf{r})$.

(2) Allow the same external current to flow through the superconductor with a pinned vortex (whose location is denoted by \mathbf{r}_0) so that the current density is asymptotically the same as that in the previous setup.

(3) Measure the local value of the magnetic field on a contour C surrounding the pinned vortex. Calculate the magnetic pressure $\mathbf{F}_{\text{mag}}(C)$ on the region surrounded by C via Eq. (6).

(4) Confirm that $|\mathbf{F}_{\text{mag}}(C)|$ is smaller than half $c(\kappa)|\mathbf{j}_{\text{tr}}(\mathbf{r}_0)||\phi_0|$. When C is sufficiently away from the core, $|\mathbf{F}_{\text{mag}}(C)|$ is close to $\frac{1}{2}c(\kappa)|\mathbf{j}_{\text{tr}}(\mathbf{r}_0)||\phi_0|$.

By showing that the magnetic pressure (Maxwell stress) does not reach the full value of the driving force, we will provide evidence that the driving force on the vortex is not purely the Lorentz force. In the above experiment, local magnetic measurements on the vortex core are unnecessary; this requires local measurements of the magnetic field on the contour in the peripheral region at a distance on the order of λ from the vortex core.

This experiment is possible using SQUID microscopy [50,51]. For example, the local magnetic field induced by the transport current $I = 10 \mu\text{A}$ was measured for a superconducting Nb film (thickness: 420 nm; width: 5 μm) at 4.2 K using SQUID-on-tip technology [50]. The measured values, which were typically 1 μT , agreed with the theoretical values. The spatial resolution, determined by the pixel size, is on the order of nanometers, which is much smaller than the penetration depth $\lambda = 105 \text{ nm}$ for Nb film at 4.2 K. The typical value of the current density in this experiment was $5 \times 10^6 \text{ A/m}^2$, which is much smaller than $j_c := \sqrt{2}B_c/(\mu_0\lambda) \sim 10^{12} \text{ A/m}^2$ (we assume that $\kappa \sim 1$ for Nb); i.e., the transport current density was much smaller than j_c . Further, the width of the film corresponds to $\ell_y/\lambda \sim 2.5$ and hence our argument is applicable. The local measurements of the magnetic field under the same transport current in the presence of a pinned vortex will yield clear evidence on the nature of the driving vortex on a quantum vortex.

C. Future issues

One future issue is the driving force on a vortex caused by a temperature gradient. In the 1960s, the Nernst effect in alloys of InPb was observed to be three orders of magnitude larger than that in the normal state [52]. This large Nernst effect has been attributed to the motion of a vortex.

For this process, the force balance relation (per unit length along the vortex axis) is given in the form [53]

$$-\sigma_\phi \nabla T + \mathbf{F}_{\text{env}} = 0 \quad (94)$$

with Eq. (4). Here, the first term represents the driving force, where s_ϕ denotes the transport entropy, which is generally different from the thermodynamic entropy. This thermal driving force is from a hotter region toward a colder region; this direction of the force can be understood from the larger entropy density around the vortex compared to that in the surrounding region [53]. The values of s_ϕ have been determined experimentally [52] and theoretically [54–58]. The theoretical and experimental results are in qualitative agreement [53]. In a theoretical paper [59], however, earlier theories [55–57] were criticized and the technical difficulty of constructing an explicit expression for the heat current operator was pointed out. Thus, the derivation of Eq. (94) for general cases and the development of a numerical algorithm for calculating the transport entropy remain open issues. The momentum balance relation and partial wave expansion adopted in the present paper will be helpful for these tasks.

The interplay between vortex motion and the spin current will be important in future spintronics. Among the emergent particles in various condensed phases, quantum vortices in superconductors are advantageous in controllability of motion by several currents, such as electric, thermal, and spin currents.

VIII. CONCLUSION

We investigated the origin of the driving force on a vortex in superconductors using the momentum flux tensor, Maxwell stress tensor, and numerical solutions of the TDGL and Maxwell equations. The numerical results show that the driving force on a rectilinear vortex in 3D superconductors is well defined only when a dissipation-free region for a flowing vortex exists in the superconductor and surrounds the vortex. We demonstrated the applicability of our results on the driving force to a flowing vortex in the generalized TDGL equation and the TDGL equation that allows for the Hall effect and a pinned vortex. We discussed the driving force on the Pearl vortex in 2D superconductors and a curved vortex in 3D superconductors.

The driving force on a quantum vortex in superconductors is neither purely hydrodynamic nor magnetic. This composite property originates from the fact that none of circulation and magnetic flux but the London's fluxoid is the topological number characterizing the vortex in superconductors.

The construction of the expression for the driving force on other types of topological object in quantum matter is a topic for future studies. The study of the driving force on a vortex in superconductors caused by a temperature gradient and the spin current is also important. The magnetic Lorentz force contributes less than half of the driving force. We proposed an experiment for confirming that the magnetic Lorentz force alone cannot account for the driving force on a vortex in superconductors.

ACKNOWLEDGMENTS

The authors thank H. Kurokawa for his useful comments on the current situation of the local measurement of magnetic fields. This work was supported by JSPS KAKENHI Grant No. 20K20891.

APPENDIX A: FORCE ON DEFORMED VORTEX

In this Appendix, we calculate the force on a curved vortex in the pinned state and discuss the force in the flow state. We show that the driving force on the pinned vortex is not purely hydrodynamic even when $\kappa \gg 1$. The equation of motion of the curved vortex was given in [30,33,35]. We assume that the deformation of the vortex line slowly varies over the scale of the dissipation region or the range of the pinning potential.

We parametrize the shape of the vortex line with $\mathbf{r} = \mathbf{r}(s)$ with s as the length along the vortex line. The region where the dissipation or pinned potential is nonzero is referred to as the core region. We model the core region as a vortex tube with a cross section of radius r_c . Outside the core region, we assume that the London equation generalized to include the effect of the vortex line holds:

$$\nabla^2 \mathbf{h}(\mathbf{r}) + \frac{\mathbf{h}(\mathbf{r})}{\lambda^2} = \frac{|\phi_0|}{\lambda^2} \int ds \frac{d\mathbf{r}(s)}{ds} \delta(\mathbf{r} - \mathbf{r}(s)). \quad (\text{A1})$$

A solution to Eq. (A1) is given by

$$\mathbf{h}_0(\mathbf{r}) = -\frac{|\phi_0|}{4\pi\lambda^2} \int ds \frac{d\mathbf{r}(s)}{ds} \frac{e^{-|r-r(s)|/\lambda}}{|\mathbf{r} - \mathbf{r}(s)|}, \quad (\text{A2})$$

from which the expression for the current density

$$\mathbf{j}_0(\mathbf{r}) = -\frac{|\phi_0|}{4\pi\mu_0\lambda^2} \nabla \times \int ds \frac{d\mathbf{r}(s)}{ds} \frac{e^{-|r-r(s)|/\lambda}}{|\mathbf{r} - \mathbf{r}(s)|} \quad (\text{A3})$$

follows. The solution to Eq. (A1) in the presence of a spatially varying transport current

$$\mathbf{j}_{\text{tr}}(\mathbf{r}) = (j_+ e^{y/\lambda} + j_- e^{-y/\lambda}) \mathbf{e}_x \quad (\text{A4})$$

is given by

$$\mathbf{h}(\mathbf{r}) = \mathbf{h}_0(\mathbf{r}) + \mathbf{h}_{\text{tr}}(\mathbf{r}) \quad (\text{A5})$$

with

$$\mathbf{h}_{\text{tr}}(\mathbf{r}) = \mu_0 \lambda (j_+ e^{y/\lambda} - j_- e^{-y/\lambda}) \mathbf{e}_z. \quad (\text{A6})$$

We assume that the vortex line varies slowly over the scale of λ ; i.e.,

$$\ell(s) := \left| \frac{d^2 \mathbf{r}(s)}{ds^2} \right|^{-1} \gg \lambda. \quad (\text{A7})$$

For a position \mathbf{r} , let $\mathbf{r}(s)$ be the closest point to the given \mathbf{r} . The magnetic field Eq. (A2) and the current density Eq. (A3) at position \mathbf{r} within the distance $r_c < |\mathbf{r} - \mathbf{r}(s)| \ll \ell(s)$ from the vortex line are those around the straight vortex line with the direction of $d\mathbf{r}(s)/ds := \mathbf{e}_{z'}$,

$$\mathbf{h}_0(\mathbf{r}) = \frac{|\phi_0|}{2\pi\lambda^2} K_0 \left(\frac{|\mathbf{r} - \mathbf{r}(s)|}{\lambda} \right) \mathbf{e}_{z'}, \quad (\text{A8})$$

$$\mathbf{j}_0(\mathbf{r}) = \frac{|\phi_0|}{2\pi\lambda^3\mu_0} K_1 \left(\frac{|\mathbf{r} - \mathbf{r}(s)|}{\lambda} \right) \mathbf{e}_{\theta'}, \quad (\text{A9})$$

with

$$\mathbf{e}_{\theta'} := \mathbf{e}_{z'} \times \frac{\mathbf{r} - \mathbf{r}(s)}{|\mathbf{r} - \mathbf{r}(s)|}. \quad (\text{A10})$$

We consider the force on a segment of the vortex line $\frac{d\mathbf{r}(s)}{ds} \Delta s$. Let $S(R)$ be the closed surface that consists of the surface

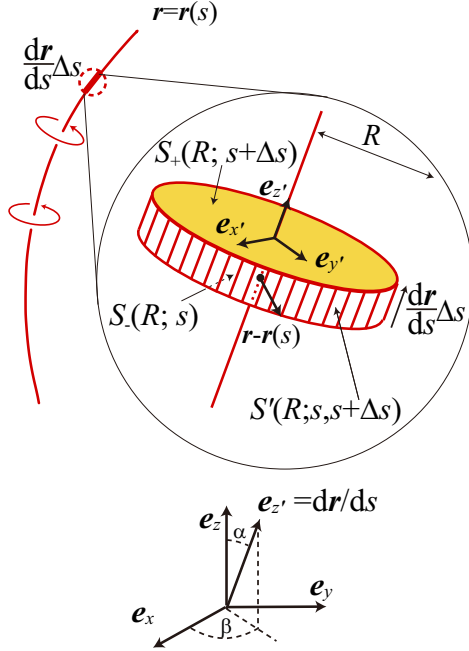


FIG. 13. Local Cartesian coordinates for the calculation of the force on a segment of the vortex line. The transport current flows in the x direction and varies along the y axis. The transport magnetic field \mathbf{h}_{tr} points along the z direction and varies along the y axis. The z' direction is parallel to the tangential direction along the vortex line at $\mathbf{r}(s)$. Here, s is the length along the vortex line. The closed surface $S = S_+(R; s + \Delta s) \cup S_-(R; s) \cup S'(R; s, s + \Delta s)$ surrounds the segment of the vortex line. The normal vector S points outward.

$S_+(R, s + \Delta s)$, bottom $S_-(R, s)$, and side $S'(R, s, s + \Delta s)$ (see Fig. 13). Here, we introduce the notation

$$S_{\pm}(R; s) = \{\mathbf{r} | \mathbf{r} \in C(R'; s); {}^{\pm}R' \in [0, R]\},$$

$$\text{with the normal vector } \mathbf{n}_{\pm} = \pm \mathbf{e}_{z'},$$

$$S'(R; s_1, s_2) = \{\mathbf{r} | \mathbf{r} \in C(R; s'); {}^{\pm}s' \in [s_1, s_2]\},$$

$$\text{with the normal vector } \mathbf{n}' = \frac{\mathbf{r} - \mathbf{r}(s)}{|\mathbf{r} - \mathbf{r}(s)|},$$

$$\text{and } C(R; s) = \left\{ \mathbf{r} | [\mathbf{r} - \mathbf{r}(s)] \perp \frac{d\mathbf{r}(s)}{ds}, |\mathbf{r} - \mathbf{r}(s)| = R \right\}.$$

We also give an explicit relation between two Cartesian coordinates:

$$\mathbf{e}_{z'} = \mathbf{e}_x s_{\alpha} c_{\beta} + \mathbf{e}_y s_{\alpha} s_{\beta} + \mathbf{e}_z c_{\alpha}, \quad (\text{A11})$$

$$\mathbf{e}_{y'} = \frac{\mathbf{e}_{z'} \times \mathbf{e}_x}{|\mathbf{e}_{z'} \times \mathbf{e}_x|} = \frac{\mathbf{e}_y c_{\alpha} - \mathbf{e}_z s_{\alpha} s_{\beta}}{\sqrt{1 - s_{\alpha}^2 c_{\beta}^2}}, \quad (\text{A12})$$

$$\begin{aligned} \mathbf{e}_{x'} &= \mathbf{e}_{y'} \times \mathbf{e}_{z'} \\ &= \frac{\mathbf{e}_x (c_{\alpha}^2 + s_{\alpha}^2 s_{\beta}^2) - \mathbf{e}_y s_{\alpha}^2 s_{\beta} c_{\beta} - \mathbf{e}_z s_{\alpha} c_{\alpha} c_{\beta}}{\sqrt{1 - s_{\alpha}^2 c_{\beta}^2}} \end{aligned} \quad (\text{A13})$$

with $s_{\alpha} = \sin \alpha$, $c_{\alpha} = \cos \alpha$, $s_{\beta} = \sin \beta$, $c_{\beta} = \cos \beta$.

First, we consider the pinned vortex and assume that $r_c = O(\xi) \ll \lambda$. We find that the hydrodynamic contribution to the momentum flow through the side surface $S'(r_c; s, s + \Delta s)$ is given by

$$\begin{aligned} & -\mu_0 \lambda^2 \int_{S'(r_c; s, s + \Delta s)} dS \left(\mathbf{j}(\mathbf{r}) \mathbf{j}(\mathbf{r}) \cdot \mathbf{n}' - \frac{\mathbf{j}(\mathbf{r})^2 \mathbf{n}'}{2} \right) \\ &= \frac{r_c}{\lambda} K_1 \left(\frac{r_c}{\lambda} \right) I_0 \left(\frac{r_c'}{\lambda} \right) \mathbf{j}_{\text{tr}}(\mathbf{r}(s)) \times \left(|\phi_0| \frac{d\mathbf{r}(s)}{ds} \Delta s \right) \end{aligned} \quad (\text{A14})$$

with

$$r_c' = r_c \sqrt{1 - s_{\alpha}^2 s_{\beta}^2}. \quad (\text{A15})$$

Here $I_m(r)$ denotes the first-kind modified Bessel function of m th order. The hydrodynamics contribution Eq. (A14) becomes

$$\mathbf{j}_{\text{tr}}(\mathbf{r}(s)) \times \left(|\phi_0| \frac{d\mathbf{r}(s)}{ds} \Delta s \right) \quad (\text{A16})$$

with the use of

$$\lim_{x \rightarrow 0} x K_1(x) I_0(x) \rightarrow 1. \quad (\text{A17})$$

The magnetic contribution to the momentum flow through the side surface is given by

$$\begin{aligned} & \frac{1}{\mu_0} \int_{S'(r_c; s, s + \Delta s)} dS \left(\mathbf{h}(\mathbf{r}) \mathbf{h}(\mathbf{r}) \cdot \mathbf{n}' - \frac{\mathbf{h}(\mathbf{r})^2 \mathbf{n}'}{2} \right) \\ &= -\Delta s \mathbf{e}_y (j_{\text{tr}}(\mathbf{r}(s)) |\phi_0|) \frac{r_c}{\lambda} K_0 \left(\frac{r_c}{\lambda} \right) I_0 \left(\frac{r_c'}{\lambda} \right) \frac{c_{\alpha}}{\sqrt{1 - s_{\alpha}^2 s_{\beta}^2}}, \end{aligned} \quad (\text{A18})$$

which is negligible when $r_c \ll \lambda$, as shown with the use of

$$\lim_{x \rightarrow 0} x K_0(x) I_0(x) \rightarrow 0. \quad (\text{A19})$$

The momentum flow through $S_+(r_c, s + \Delta s)$ and $S_-(r_c, s)$ cannot be directly calculated, because these surfaces belong to the core region, where the London equation is not applicable. However, we can show that these contributions are negligible when $r_c \ll \lambda$.

The electromagnetic fields are bounded in the core region and thus the magnetic contribution to the momentum flow through $S_+(r_c, s + \Delta s)$ and $S_-(r_c, s)$ is proportional to r_c^2 and thus $O((r_c/\lambda)^2)$, which is negligible when $r_c \ll \lambda$.

To estimate the hydrodynamic contribution to the momentum flow through $S_+(r_c, s + \Delta s)$ and $S_-(r_c, s)$, we assume that the Ginzburg-Landau theory holds in the core region and that the momentum flux tensor has the form Eq. (26) (note that the form of the momentum flux tensor of the equilibrium Ginzburg-Landau equation is the same as that for the TDGL equation). Among the factors in $\mathcal{P}_{\mu\nu}$, only \mathbf{Q}_0 ($=\mathbf{Q}$ in the absence of a transport current) can be singular. In the case discussed in this Appendix, $\mathbf{Q}_0 \propto 1/|\mathbf{r} - \mathbf{r}(s)|$. The net contribution to the momentum flow comes from the terms $O(j_{\text{tr}})$ and thus the singularity relevant to our calculation comes from at most $\mathbf{Q}_0 \mathbf{Q}_1 \propto 1/|\mathbf{r} - \mathbf{r}(s)|$. Here, $\mathbf{Q}_1 = \mathbf{Q} - \mathbf{Q}_0$. Thus, the hydrodynamic contribution to the momentum flow through $S_+(r_c, s + \Delta s)$ and $S_-(r_c, s)$ is proportional to r_c and thus $O(r_c/\lambda)$, which is also negligible when $r_c \ll \lambda$.

We find that the driving force on the segment of the vortex line through the surface $S(r_c)$ is given by Eq. (A16) with the accuracy $O((r_c/\lambda))$. The hydrodynamic contribution through the side surface is dominant. When we consider momentum flow through $S(R; s)$, $S_+(R; s + \Delta s)$, and $S_-(R; s)$, the bottom as well as side $S'(R; s, s + \Delta s)$ contribute. The resultant force, as expected, is the same as Eq. (A16) but the relative contribution depends on R . The magnetic contribution is given by

$$\mathbf{F}_{\text{mag}}(R) = \frac{RK_0\left(\frac{R}{\lambda}\right)I_1\left(\frac{R'}{\lambda}\right)}{\lambda\sqrt{1-s_\alpha^2s_\beta^2}} \mathbf{j}_{\text{tr}}(\mathbf{r}(s)) \times \left(|\phi_0| \frac{d\mathbf{r}(s)}{ds} \Delta s \right) + \mathbf{F}'(R), \quad (\text{A20})$$

where $\mathbf{F}'(R)$ is zero when $s_\alpha s_\beta = 0$, otherwise

$$\mathbf{F}'(R) = -\frac{e_z \mathbf{j}_{\text{tr}}(\mathbf{r}(s)) |\phi_0| \Delta s}{s_\alpha s_\beta} \times \left[\frac{R}{\lambda} K_1\left(\frac{R}{\lambda}\right) I_0\left(\frac{R'}{\lambda}\right) + \frac{R}{\lambda\sqrt{1-s_\alpha^2s_\beta^2}} \times K_0\left(\frac{R}{\lambda}\right) I_1\left(\frac{R'}{\lambda}\right) - 1 \right]. \quad (\text{A21})$$

The hydrodynamic contribution to the force on the segment is

$$\mathbf{F}_{\text{hydro}}(R) = \mathbf{j}_{\text{tr}}(\mathbf{r}(s)) \times \left(|\phi_0| \frac{d\mathbf{r}(s)}{ds} \Delta s \right) - \frac{RK_0\left(\frac{R}{\lambda}\right)I_1\left(\frac{R'}{\lambda}\right)}{\lambda\sqrt{1-s_\alpha^2s_\beta^2}} \mathbf{j}_{\text{tr}}(\mathbf{r}(s)) \times \left(|\phi_0| \frac{d\mathbf{r}(s)}{ds} \Delta s \right) - \mathbf{F}'(R). \quad (\text{A22})$$

When $s_\alpha s_\beta = 0$, i.e., the vortex is perpendicular to the transport current, the two contributions respectively become

$$\mathbf{F}_{\text{hydro}}(R) = \mathbf{j}_{\text{tr}}(\mathbf{r}(s)) \times \left(|\phi_0| \frac{d\mathbf{r}(s)}{ds} \Delta s \right) \left(1 - \frac{RK_0\left(\frac{R}{\lambda}\right)I_1\left(\frac{R'}{\lambda}\right)}{\lambda} \right), \quad (\text{A24})$$

$$\mathbf{F}_{\text{mag}}(R) = \mathbf{j}_{\text{tr}}(\mathbf{r}(s)) \times \left(|\phi_0| \frac{d\mathbf{r}(s)}{ds} \Delta s \right) \frac{RK_0\left(\frac{R}{\lambda}\right)I_1\left(\frac{R'}{\lambda}\right)}{\lambda}. \quad (\text{A25})$$

In this case, each force has the proper direction and the relative weight depends on R . When $s_\alpha s_\beta \neq 0$ (the segment of the vortex line is not perpendicular to the transport current), the term $\mathbf{F}'(R)$ is nonzero and none of them has the proper direction. This demonstrates that only the sum of the two forces is physically meaningful as the driving force on the segment of the vortex line. In other words, the driving force on the vortex segment is not purely hydrodynamic or magnetic.

In the derivation of $\mathbf{F}(r_c)$, the evaluation of the contribution of the momentum flow through $S_+(r_c; s + \Delta s)$ and $S_-(r_c; s)$ requires an argument beyond the London equation. For the pinned vortex, these contributions are found be negligible due

to the smallness of r_c/λ . For the flow vortex, $r_c/\lambda = O(1)$, and thus the same argument in the derivation of $\mathbf{F}(r_c)$ is not directly applicable. Further discussion regarding the core region is required.

APPENDIX B: PEARL VORTEX

1. Pearl's solution

In this Appendix, we summarize the derivation of the vector potential Eq. (64), current density Eq. (66), and magnetic field [Eqs. (68) and (69)] for a single vortex in a 2D superconductor in the absence of a transport current. The outline of this Appendix is based on [23,38]. However, the current density Eq. (66) and magnetic field [Eqs. (68) and (69)] for all distances from the vortex were not given in these references. We derive them as a prerequisite for calculating the force on a vortex in Appendix B.

First, we define the Fourier transform of $\mathbf{A}(\mathbf{r})$ as

$$\mathbf{A}(\mathbf{q}) = \int_{3\text{D}} \mathbf{A}(\mathbf{r}) e^{-i\mathbf{q}\cdot\mathbf{r}} d\mathbf{r}, \quad (\text{B1})$$

from which

$$\mathbf{A}(\mathbf{r}) = \int_{3\text{D}} \mathbf{A}(\mathbf{q}) e^{i\mathbf{q}\cdot\mathbf{r}} \frac{d\mathbf{q}}{(2\pi)^3} \quad (\text{B2})$$

follows. Both sides of Eq. (52) are multiplied by $e^{-i(\mathbf{q}_\perp \cdot \mathbf{r}_\perp + q_z z)}$ and then integrated with respect to \mathbf{r} over the 3D space. We then obtain

$$-(q_\perp^2 + q_z^2) \mathbf{A}(\mathbf{q}) = \frac{2}{\lambda_{\text{eff}}} \left(-\Phi_{2\text{D}}(\mathbf{q}_\perp) + \int_{-\infty}^{\infty} \mathbf{A}(\mathbf{q}) \frac{dq_z}{2\pi} \right) \quad (\text{B3})$$

with

$$\Phi_{2\text{D}}(\mathbf{q}_\perp) = \int_{2\text{D}} d\mathbf{r}_\perp e^{-i\mathbf{q}_\perp \cdot \mathbf{r}_\perp} \frac{\hbar}{e^*} \mathbf{e}_z \times \frac{\mathbf{r}_\perp}{r_\perp^2} = \frac{\hbar}{e^*} \mathbf{e}_z \times \frac{-2\pi i \mathbf{q}_\perp}{q_\perp^2}. \quad (\text{B4})$$

We set

$$\int_{-\infty}^{\infty} \mathbf{A}(\mathbf{q}) \frac{dq_z}{2\pi} = 2\pi \lambda_{\text{eff}} \mathbf{K}_s(\mathbf{q}_\perp) \quad (\text{B5})$$

and derive $\mathbf{K}_s(\mathbf{q}_\perp)$. Dividing Eq. (B3) by $-(q_\perp^2 + q_z^2)$ yields

$$\mathbf{A}(\mathbf{q}) = \frac{2[\Phi_{2\text{D}}(\mathbf{q}_\perp) - 2\pi \lambda_{\text{eff}} \mathbf{K}_s(\mathbf{q}_\perp)]}{(q_\perp^2 + q_z^2) \lambda_{\text{eff}}}. \quad (\text{B6})$$

After integrating the above equation with respect to q_z , it follows that

$$2\pi \lambda_{\text{eff}} \mathbf{K}_s(\mathbf{q}_\perp) = \frac{1}{q_\perp} \left(\frac{\Phi_{2\text{D}}(\mathbf{q}_\perp)}{\lambda_{\text{eff}}} - 2\pi \mathbf{K}_s(\mathbf{q}_\perp) \right), \quad (\text{B7})$$

which yields

$$\mathbf{K}_s(\mathbf{q}_\perp) = \frac{\Phi_{2\text{D}}(\mathbf{q}_\perp)}{2\pi \lambda_{\text{eff}} (1 + \lambda_{\text{eff}} q_\perp)} \quad (\text{B8})$$

$$= \frac{\hbar}{e^* \lambda_{\text{eff}}} \mathbf{e}_z \times \frac{-i \mathbf{q}_\perp}{(1 + \lambda_{\text{eff}} q_\perp) q_\perp^2}. \quad (\text{B9})$$

From Eqs. (B6) and (B8),

$$\mathbf{A}(\mathbf{q}) = \frac{2q_\perp \Phi_{2\text{D}}(\mathbf{q}_\perp)}{(q_\perp^2 + q_z^2) (1 + \lambda_{\text{eff}} q_\perp)} \quad (\text{B10})$$

follows. We then perform the inverse Fourier transform

$$\begin{aligned} \mathbf{A}(\mathbf{r}_\perp, z) &= \int \frac{d\mathbf{q}_\perp}{(2\pi)^2} e^{i\mathbf{q}_\perp \cdot \mathbf{r}_\perp} \int \frac{dq_z}{2\pi} e^{iq_z z} \mathbf{A}(\mathbf{q}) \\ &= \int \frac{dq_\perp}{(2\pi)^2} e^{i\mathbf{q}_\perp \cdot \mathbf{r}_\perp} \frac{e^{-q_\perp |z|} \Phi_{2D}(\mathbf{q}_\perp)}{(1 + \lambda_{\text{eff}} q_\perp)} \\ &= -\frac{2\pi i \hbar e_z}{e^*} \times \int \frac{dq_\perp}{(2\pi)^2} e^{i\mathbf{q}_\perp \cdot \mathbf{r}_\perp} \frac{\mathbf{q}_\perp}{q_\perp} \frac{e^{-q_\perp |z|}}{(1 + \lambda_{\text{eff}} q_\perp) q_\perp} \\ &\equiv \mathbf{e}_\theta A(r_\perp, z) \end{aligned} \quad (\text{B11})$$

with

$$A(r_\perp, z) = |\phi_0| \int_0^\infty \frac{dq_\perp}{2\pi} \frac{e^{-q_\perp |z|} J_1(q_\perp r_\perp)}{(1 + \lambda_{\text{eff}} q_\perp)},$$

which is Eq. (64) in the main text. The magnetic field $\mathbf{h}(\mathbf{r}_\perp, z) = h_r(\mathbf{r}_\perp, z) \mathbf{e}_{r_\perp} + h_z(\mathbf{r}_\perp, z) \mathbf{e}_z = \nabla \times \mathbf{A}$ is given by

$$\begin{aligned} h_z(\mathbf{r}_\perp, z) &= \frac{1}{r_\perp} \frac{\partial(r_\perp A(r_\perp, z))}{\partial r_\perp} \\ &= |\phi_0| \int_0^\infty \frac{dq_\perp}{2\pi} \frac{e^{-q_\perp |z|} q_\perp J_0(q_\perp r_\perp)}{(1 + \lambda_{\text{eff}} q_\perp)}, \end{aligned} \quad (\text{B13})$$

$$\begin{aligned} h_{r_\perp}(\mathbf{r}_\perp, z) &= -\frac{\partial(r_\perp A(r_\perp, z))}{\partial z} \\ &= |\phi_0| \text{sgn}(z) \int_0^\infty \frac{dq_\perp}{2\pi} \frac{e^{-q_\perp |z|} q_\perp J_1(q_\perp r_\perp)}{(1 + \lambda_{\text{eff}} q_\perp)}. \end{aligned} \quad (\text{B14})$$

In the second equality in Eq. (B13), we use the recursive formula of the Bessel functions. The derivatives of Eqs. (B13) and (B14),

$$\begin{aligned} \frac{\partial h_z(\mathbf{r}_\perp, z)}{\partial r_\perp} &= |\phi_0| \int_0^\infty \frac{dq_\perp}{2\pi} \frac{e^{-q_\perp |z|} q_\perp}{(1 + \lambda_{\text{eff}} q_\perp)} \frac{\partial J_0(q_\perp r_\perp)}{\partial r_\perp} \\ &= -|\phi_0| \int_0^\infty \frac{dq_\perp}{2\pi} \frac{e^{-q_\perp |z|} q_\perp^2 J_1(q_\perp r_\perp)}{(1 + \lambda_{\text{eff}} q_\perp)}, \end{aligned} \quad (\text{B15})$$

$$\begin{aligned} \frac{\partial h_r(\mathbf{r}_\perp, z)}{\partial z} &= 2|\phi_0| \delta(z) \int_0^\infty \frac{dq_\perp}{2\pi} \frac{e^{-q_\perp |z|} q_\perp J_1(q_\perp r_\perp)}{(1 + \lambda_{\text{eff}} q_\perp)} \\ &\quad - |\phi_0| \int_0^\infty \frac{dq_\perp}{2\pi} \frac{e^{-q_\perp |z|} q_\perp^2 J_1(q_\perp r_\perp)}{(1 + \lambda_{\text{eff}} q_\perp)}, \end{aligned} \quad (\text{B16})$$

lead to the current density

$$\mathbf{j}(\mathbf{r}_\perp, z) = \delta(z) \mathbf{e}_\theta j_{2D}(\mathbf{r}_\perp),$$

with

$$\begin{aligned} j_{2D}(\mathbf{r}_\perp) &= \frac{2|\phi_0|}{\mu_0} \int_0^\infty \frac{dq_\perp}{2\pi} \frac{q_\perp J_1(q_\perp r_\perp)}{(1 + \lambda_{\text{eff}} q_\perp)} \\ &= \frac{|\phi_0|}{\pi \mu_0 \lambda_{\text{eff}}^2} \left[\frac{\lambda_{\text{eff}}}{r_\perp} - \vartheta\left(\frac{r_\perp}{\lambda_{\text{eff}}}\right) \right]. \end{aligned} \quad (\text{B17})$$

Here, the relation Eq. (67) is used in the last equality. This expression for the current density is Eq. (66) in the main text. Equation (68) for $h_{r_\perp}(r_\perp, z \rightarrow \pm 0)$ in the main text results from Eq. (B14) in the limit $z \rightarrow \pm 0$ and Eq. (67). Equation

(69) for $h_z(r_\perp, 0)$ in the main text results from Eq. (B14) in the limit $z \rightarrow \pm 0$, and Eq. (70).

2. Derivation of expression Eq. (78) for $F_{\text{hydro}}(S)$

From symmetry, Eq. (76) is nonzero only for $\mu = y$ and only $O(j_{\text{tr}})$ terms contribute to the integral. We obtain

$$\begin{aligned} F_{\text{hydro}}(S) &= -\mathbf{e}_y \int_{S'} dS \mathcal{P}_{yv} \mathbf{e}_v \cdot \mathbf{e}_{r_\perp} = -\mathbf{e}_y \mu_0 \lambda^2 \\ &\quad \times \int_{S'} dS [j_y(\mathbf{r}_\perp, z) \mathbf{j}(\mathbf{r}_\perp, z) \cdot \mathbf{e}_{r_\perp} \\ &\quad - \frac{\mathbf{j}(\mathbf{r}_\perp, z)^2}{2} \mathbf{e}_y \cdot \mathbf{e}_{r_\perp}]. \end{aligned} \quad (\text{B18})$$

In the first term in the integrand in the last line, $\mathbf{j}(\mathbf{r}_\perp, z)$, comes only from $\mathbf{j}_{\text{Pearl}}(\mathbf{r}_\perp, z)$ and thus

$$\int_{S'} dS j_y(\mathbf{r}_\perp, z) \mathbf{j}(\mathbf{r}_\perp, z) \cdot \mathbf{e}_{r_\perp} \quad (\text{B19})$$

$$= \int_{S'} dS \{[\mathbf{j}_{\text{Pearl}}(\mathbf{r}_\perp, z) \cdot \mathbf{e}_y] (\mathbf{j}_{\text{tr}} \cdot \mathbf{e}_{r_\perp})\}$$

$$= \oint d\ell [j_{2D}(R)/d] (j_{\text{tr}}/d) \cos^2 \theta. \quad (\text{B20})$$

In the last equality, we use Eqs. (77a) and (77b). The contribution in the second term in the integrand in the last line in Eq. (B18) becomes

$$\begin{aligned} & - \int_{S'} dS \left[\frac{\mathbf{j}(\mathbf{r}_\perp, z)^2}{2} \mathbf{e}_y \cdot \mathbf{e}_{r_\perp} \right] \\ &= \int_{S'} dS [\mathbf{j}_{\text{Pearl}}(\mathbf{r}_\perp, z) \cdot \mathbf{j}_{\text{tr}}(\mathbf{r}_\perp, z) \sin \theta] \\ &= d \oint d\ell [j_{2D}(R)/d] (j_{\text{tr}}/d) \sin^2 \theta. \end{aligned} \quad (\text{B21})$$

From Eqs. (B20), (B21), and (66), it follows that

$$\begin{aligned} & \int_{S'} dS \left[j_y(\mathbf{r}_\perp, z) \mathbf{j}(\mathbf{r}_\perp, z) \cdot \mathbf{e}_{r_\perp} - \frac{\mathbf{j}(\mathbf{r}_\perp, z)^2}{2} \mathbf{e}_y \cdot \mathbf{e}_{r_\perp} \right] \\ &= \frac{2\pi R j_{\text{tr}} j_{2D}(R)}{d} = \frac{2|\phi_0|}{\underbrace{d \mu_0 \lambda_{\text{eff}}}_{|\phi_0|/(\mu_0 \lambda^2)}} \left[1 - \frac{R}{\lambda_{\text{eff}}} \vartheta\left(\frac{R}{\lambda_{\text{eff}}}\right) \right]. \end{aligned} \quad (\text{B22})$$

Substituting the expression in the last line into Eq. (B18), we obtain the expression Eq. (78) for $F_{\text{hydro}}(S)$.

3. Derivation of Eq. (79) for $F_{\text{mag}}(S)$

From symmetry, we see that Eq. (55) is nonzero only for $\mu = y$ and only $O(j_{\text{tr}})$ terms contribute to the integral.

First, we consider the contribution from S_+ , where the normal vector \mathbf{n} is \mathbf{e}_z and the \mathbf{h}^2 term in the integrand in Eq. (55) does not contribute. We can thus write

$$\int_{S_+} dS \mathcal{T}_{yv} n_v = \frac{1}{\mu_0} \int_{S_+} dS h_y(\mathbf{r}_\perp, +0) h_z(\mathbf{r}_\perp, +0). \quad (\text{B23})$$

In the integrand, $h_z(\mathbf{r}_\perp, +0)$ comes only from $\mathbf{h}_{\text{Pearl}}(\mathbf{r}_\perp, +0)$ and thus we replace the other factor, namely $h_y(\mathbf{r}_\perp, +0)$, in

the integrand by $h_{\text{tr}}(\mathbf{r}_{\perp}, +0) = -\mu_0 j_{\text{tr}} d/2$; i.e.,

$$\begin{aligned} \int_{S_+} dS \mathcal{T}_{y\nu} n_{\nu} &= -\frac{j_{\text{tr}} d}{2} \int_{S_+} dS h_z(\mathbf{r}_{\perp}, 0) \\ &= -\frac{j_{\text{tr}} |\phi_0| d}{2\lambda_{\text{eff}}^2} \int_0^R dr_{\perp} r_{\perp} \varpi\left(\frac{r_{\perp}}{\lambda_{\text{eff}}}\right). \end{aligned} \quad (\text{B24})$$

In the last equality, we use Eq. (69). The integration in the last line is performed with the relation Eq. (70) between ϖ and ϑ as

$$\begin{aligned} \int_{S_+} dS \mathcal{T}_{y\nu} n_{\nu} &= -\frac{j_{\text{tr}} |\phi_0| d}{2} [x\vartheta(x)]_{\xi/\lambda_{\text{eff}}}^{R/\lambda_{\text{eff}}} \\ &= -\frac{j_{\text{tr}} |\phi_0| d}{2} \left(\frac{R}{\lambda_{\text{eff}}}\right) \vartheta\left(\frac{R}{\lambda_{\text{eff}}}\right). \end{aligned} \quad (\text{B25})$$

The contribution from S_- to $\mathbf{F}_{\text{mag}}(S)$ is the same as that from S_+ because \mathbf{n} on S_- is the minus of the \mathbf{n} on S_+ and $h_y(\mathbf{r}_{\perp}, -0) = -h_y(\mathbf{r}_{\perp}, +0)$.

Last, we show that the contribution from S' to $\mathbf{F}_{\text{mag}}(S)$ is $j_{\text{tr}} |\phi_0| d \times O(d/\lambda_{\text{eff}})$, which is negligible compared to that from S_{\pm} to $\mathbf{F}_{\text{mag}}(S)$. Considering that (i) the normal vector on S' is $\mathbf{e}_{r\perp}$ and (ii) the $O(j_{\text{tr}})$ terms contribute to the integral, we

see that

$$\begin{aligned} \int_{S'} dS \mathcal{T}_{y\nu} n_{\nu} &= \frac{1}{\mu_0} \int_{S'} dS (h_y(\mathbf{r}_{\perp}, z) \mathbf{h}(\mathbf{r}_{\perp}, z) \cdot \mathbf{e}_{r\perp} \\ &\quad - \frac{1}{2} \mathbf{h}(\mathbf{r}_{\perp}, z)^2 \mathbf{e}_{r\perp} \cdot \mathbf{e}_y) \\ &= \frac{1}{\mu_0} \int_{S'} dS [\mathbf{h}_{\text{tr}}(\mathbf{r}_{\perp}, z) \cdot \mathbf{e}_y] [\mathbf{h}_{\text{Pearl}}(\mathbf{r}_{\perp}, z) \cdot \mathbf{e}_{r\perp}] \\ &\quad + \frac{1}{\mu_0} \int_{S'} dS [\mathbf{h}_{\text{Pearl}}(\mathbf{r}_{\perp}, z) \cdot \mathbf{e}_y] [\mathbf{h}_{\text{tr}}(\mathbf{r}_{\perp}, z) \cdot \mathbf{e}_{r\perp}] \end{aligned} \quad (\text{B26})$$

$$- \frac{1}{\mu_0} \int_{S'} dS [\mathbf{h}_{\text{tr}}(\mathbf{r}_{\perp}, z) \cdot \mathbf{h}_{\text{Pearl}}(\mathbf{r}_{\perp}, z)] (\mathbf{e}_{r\perp} \cdot \mathbf{e}_y) \quad (\text{B27})$$

$$= \frac{1}{\mu_0} \int_{S'} dS [\mathbf{h}_{\text{tr}}(\mathbf{r}_{\perp}, z) \cdot \mathbf{e}_y] [\mathbf{h}_{\text{Pearl}}(\mathbf{r}_{\perp}, z) \cdot \mathbf{e}_{r\perp}] \quad (\text{B28})$$

$$= -\frac{j_{\text{tr}} |\phi_0| d}{2} \left(1 - \frac{R}{\lambda_{\text{eff}}}\right) \vartheta\left(\frac{R}{\lambda_{\text{eff}}}\right) \times \frac{d}{\lambda_{\text{eff}}}. \quad (\text{B29})$$

In the course of calculation, note that the two lines Eqs. (B26) and (B27) cancel each other. In the last equality, we use Eqs. (62) and (68). We confirm that the contribution from S' is negligible compared to that from S_{\pm} . The sum of the contributions from S_{\pm} to $\mathbf{F}_{\text{mag}}(S)$ is twice Eq. (B23) and we arrive at Eq. (79).

-
- [1] Y. Cao, V. Fatemi, S. Fang, K. Watanabe, T. Taniguchi, E. Kaxiras, and P. Jarillo-Herrero, *Nature (London)* **556**, 43 (2018).
- [2] T. Machida, Y. Sun, S. Pyon, S. Takeda, Y. Kohsaka, T. Hanaguri, T. Sasagawa, and T. Tamegai, *Nat. Mater.* **18**, 811 (2019).
- [3] J. Linder and J. W. A. Robinson, *Nat. Phys.* **11**, 307 (2015).
- [4] D. A. Ivanov, *Phys. Rev. Lett.* **86**, 268 (2001).
- [5] V. L. Berezinskii, *Zh. Eksp. Teor. Fiz.* **59**, 907 (1970) [*Sov. Phys. JETP* **32**, 493 (1971)].
- [6] J. M. Kosterlitz and D. J. Thouless, *J. Phys. C* **6**, 1181 (1973).
- [7] B. I. Halperin and D. R. Nelson, *J. Low Temp. Phys.* **36**, 599 (1979).
- [8] S. Doniach and B. A. Huberman, *Phys. Rev. Lett.* **42**, 1169 (1979).
- [9] A. Vargunin and M. Silaev, *Sci. Rep.* **9**, 5914 (2019).
- [10] T. Taira, Y. Kato, M. Ichioka, and H. Adachi, *Phys. Rev. B* **103**, 134417 (2021).
- [11] P. G. de Gennes and J. Matricon, *Rev. Mod. Phys.* **36**, 45 (1964).
- [12] J. Bardeen, *Phys. Rev. Lett.* **13**, 747 (1964).
- [13] M. J. Stephen and J. Bardeen, *Phys. Rev. Lett.* **14**, 112 (1965).
- [14] H. Suhl, *Phys. Rev. Lett.* **14**, 226 (1965).
- [15] J. Bardeen and M. J. Stephen, *Phys. Rev.* **140**, A1197 (1965).
- [16] P. Nozières and W. F. Vinen, *Philos. Mag.* **14**, 667 (1966).
- [17] P. Ao and D. J. Thouless, *Phys. Rev. Lett.* **70**, 2158 (1993).
- [18] E. B. Sonin, *Phys. Rev. B* **55**, 485 (1997).
- [19] D. X. Chen, J. J. Moreno, A. Hernando, A. Sanchez, and B. Z. Li, *Phys. Rev. B* **57**, 5059 (1998).
- [20] O. Narayan, *J. Phys. A* **36**, L373 (2003).
- [21] Y. Kato and C.-K. Chung, *J. Phys. Soc. Jpn.* **85**, 033703 (2016).
- [22] Y. B. Kim and M. J. Stephen, in *Superconductivity*, edited by R. D. Parks (Marcel Dekker Inc., New York, 1969), Vol. 2.
- [23] P. G. de Gennes, *Superconductivity of Metals and Alloys* (Benjamin Inc., New York, 1966).
- [24] D. Saint-James, G. Sarma, and E. J. Thomas, *Type II Superconductivity* (Pergamon Press, Oxford, 1969).
- [25] M. Tinkham, *Introduction to Superconductivity* (McGraw-Hill, New York, 1996), 2nd ed.
- [26] D. R. Tilley and J. Tilley, *Superfluidity and Superconductivity* (Adam Hilger Ltd., Bristol, 1986), 2nd ed.
- [27] A. A. Abrikosov, *Fundamentals of the Theory of Metals* (Elsevier Science Publishers, Amsterdam, 1988).
- [28] N. B. Kopnin, *Theory of Nonequilibrium Superconductivity* (Oxford University Press, Oxford, 2001).
- [29] G. Blatter, M. V. Feigel'man, V. B. Geshkenbein, A. I. Larkin, and V. M. Vinokur, *Rev. Mod. Phys.* **66**, 1125 (1994).
- [30] L. P. Gor'kov and N. B. Kopnin, *Zh. Eksp. Teor. Fiz.* **60**, 2331 (1971) [*Sov. Phys. JETP* **33**, 1251 (1971)].
- [31] L. P. Gor'kov and N. B. Kopnin, *Zh. Eksp. Teor. Fiz.* **64**, 356 (1973) [*Sov. Phys. JETP* **37**, 183 (1973)].
- [32] L. P. Gor'kov and N. B. Kopnin, *Zh. Eksp. Teor. Fiz.* **65**, 396 (1973) [*Sov. Phys. JETP* **38**, 195 (1974)].
- [33] L. P. Gor'kov and N. B. Kopnin, *Usp. Fiz. Nauk* **116**, 413 (1975) [*Sov. Phys. Usp.* **18**, 496 (1976)].
- [34] A. I. Larkin and Yu. N. Ovchinnikov, in *Nonequilibrium Superconductivity*, edited by D. N. Langenberg and A. I. Larkin (Elsevier, Amsterdam, 1986).
- [35] A. T. Dorsey, *Phys. Rev. B* **46**, 8376 (1992).

- [36] N. B. Kopnin, B. I. Ivlev, and V. A. Kalatsky, *J. Low Temp. Phys.* **90**, 1 (1993).
- [37] J. Friedel, P. G. de Gennes, and J. Matricon, *Appl. Phys. Lett.* **2**, 119 (1963).
- [38] J. Pearl, *Appl. Phys. Lett.* **15**, 65 (1964).
- [39] F. London, *Superfluids* (Wiley, New York, 1950), Vol. I.
- [40] A. Schmid, *Phys. kondens. Mater.* **5**, 302 (1966).
- [41] L. P. Gor'kov and G. M. Éliashberg, *Zh. Eksp. Teor. Fiz.* **54**, 612 (1968) [*Sov. Phys. JETP* **27**, 328 (1968)].
- [42] See Supplemental Material at <http://link.aps.org/supplemental/10.1103/PhysRevB.104.064516> for details of reduction to one-dimensional problem in each partial wave and the numerical methods.
- [43] C. R. Hu and R. S. Thompson, *Phys. Rev. B* **6**, 110 (1972).
- [44] A. L. Fetter and P. C. Hohenberg, in *Superconductivity*, edited by R. D. Parks (Marcel Dekker Inc., New York, 1969), Vol. 2.
- [45] B. V. Svistunov, E. S. Babaev, and N. V. Prokof'ev, *Superfluid States of Matter* (CRC Press, 2015), Sec. 5.4.2.
- [46] A. G. van Vijeijken, *Philips Res. Rep., Suppl.* **8**, 1 (1968).
- [47] R. Watts-Tobin, Y. Krähenbühl, and L. Kramer, *J. Low Temp. Phys.* **42**, 459 (1981).
- [48] A. G. van Vijeijken and A. K. Niessen, *Philips Res. Rep.* **20**, 505 (1965).
- [49] N. D. Mermin and T.-L. Ho, *Phys. Rev. Lett.* **36**, 594 (1976).
- [50] D. Vasyukov, Y. Anahory, L. Embon, D. Halbertal, J. Cuppens, L. Neeman, A. Finkler, Y. Segev, Y. Myasoedov, M. L. Rappaport, M. E. Huber, and E. Zeldov, *Nat. Nanotechnol.* **8**, 639 (2013).
- [51] J. R. Kirtley, L. Paulius, A. J. Rosenberg, J. C. Palmstrom, C. M. Holland, E. M. Spanton, D. Schiess, C. L. Jermain, J. Gibbons, Y.-K.-K. Fung, M. E. Huber, D. C. Ralph, M. B. Ketchen, G. W. Gibson Jr., and K. A. Moler, *Rev. Sci. Instrum.* **87**, 093702 (2016).
- [52] F. A. Otter Jr. and P. R. Solomon, *Phys. Rev. Lett.* **16**, 681 (1966).
- [53] R. P. Huebener, *Magnetic Flux Structures in Superconductors* (Springer, Berlin, 1979), Chap. 9.
- [54] M. J. Stephen, *Phys. Rev. Lett.* **16**, 801 (1966).
- [55] K. Maki, *J. Low Temp. Phys.* **1**, 45 (1969).
- [56] A. Houghton and K. Maki, *Phys. Rev. B* **3**, 1625 (1971).
- [57] O. L. de Lange, *J. Phys. F: Met. Phys.* **4**, 1222 (1974).
- [58] N. B. Kopnin, *Zh. Eksp. Teor. Fiz.* **69**, 364 (1975) [*Sov. Phys. JETP* **42**, 186 (1976)].
- [59] N. B. Kopnin, *J. Low Temp. Phys.* **93**, 117 (1993).